Recent tests of the mode-coupling theory for glassy dynamics

1999 J. Phys.: Condens. Matter 11 A1

(http://iopscience.iop.org/0953-8984/11/10A/002)

J. Phys.: Condens. Matter **11** (1999) A1–A45. Printed in the UK PII: S0953-8984(99)00262-3

REVIEW ARTICLE

Recent tests of the mode-coupling theory for glassy dynamics

Wolfgang Götze

Physik-Department, Technische Universität München, D-85747 Garching, Germany

Received 2 October 1998

Abstract. An overview is given of recent tests of the mode-coupling theory for the evolution of structural relaxation in glass-forming liquids. Emphasis is put on comparisons between the leading-order asymptotic formulae derived for the dynamics near glass transition singularities and the results of neutron scattering, depolarized light scattering, impulsive stimulated light scattering and dielectric-loss spectroscopy for conventional liquids. The tests based on photon-correlation spectroscopy results for the glassy dynamics of colloids and the findings of molecular dynamics simulations for model systems are also considered.

1. Introduction

The mode-coupling theory for the density-fluctuation dynamics of simple liquids was developed originally in order to deal with the cage effect. This effect has been known of for some time as the essential feature distinguishing the dynamics of a liquid from that of a dense gas. It was discovered that the derived equations of motion, which deal with a self-consistent treatment of density-fluctuation propagation and current relaxations, lead to a bifurcation of the long-time limit of the density correlators. This bifurcation provided a model for an ideal liquid-to-glass transition. The identification of this glass transition singularity opened up the possibility for an analytic solution of the complicated non-linear equations by means of asymptotic expansions using the distance from the transition point as a small parameter. It turned out that the bifurcation is connected with a novel dynamical scenario. A set of predictions were produced concerning, e.g., fractal decay laws and unconventional dynamical scaling. The crucial point was the suggestion that the evolution of glassy dynamics manifests itself in a dynamical window of several-orders-of-magnitude variations of time t or frequency ω adjacent to the short-time or high-frequency regime, respectively, where conventional condensed-matter dynamics is observed. Thus the mode-coupling theory for the evolution of glassy dynamics (MCT) provided motivation for studies of the dynamical regime indicated.

Neutron spin–echo spectroscopy demonstrated [1] that a molten mixed salt does indeed exhibit the so-called α-relaxation process at temperatures far above the glass transition on the ns timescale, i.e. on a timescale which is several orders of magnitude smaller than the one for which it was analysed by the pioneers of glass transition research. It was found in addition that the scattering cross sections for neutrons [2] and light [3] exhibit within the GHz window a so-called critical spectrum, i.e. the predicted self-similar spectral enhancement above the white-noise background. Incoherent and coherent neutron scattering spectroscopy of a van der Waals liquid detected an anomaly for the so-called non-ergodicity parameters and this was used to show that the evolution of glassy dynamics is connected with a crossover temperature

0953-8984/99/SA0001+45$19.50

T_c, which is located about 47 K above the calorimetric glass transition temperature T_g and about 39 K below the melting temperature T_m [4, 5]. Molecular dynamics simulations [6–8] corroborated these findings and provided evidence for the factorization of spatial and temporal correlations for density fluctuations in an intermediate-time window, a property which is not found for normal-liquid dynamics nor for conventional phase transition phenomena. A number of polymers were identified whose dielectric-loss spectra could be interpreted with the MCT scaling laws [9], a finding supporting the predicted universality features. It was discovered that a slightly polydisperse colloid of hard spheres exhibits an equilibrium transition at some critical density from an ergodic liquid to a non-ergodic solid [10], thereby demonstrating that complexity of the system is irrelevant for the existence of a glass transition.

The work described in the preceding paragraph has been reviewed in reference [11], and therefore this material will not be considered further in the following. During the past seven years an impressive increase in the amount of research on the evolution of glassy dynamics has occurred. Neutron scattering studies have been refined and extended to additional systems. The dynamical window of molecular dynamics studies was extended by more than an order of magnitude and the data statistics was improved. The window accessible to impulsive stimulated light scattering spectroscopy was enlarged with the result that the elastic modulus could be determined for frequencies up to 1 GHz. Studies of colloid dynamics were extended, so the glass transition for the hard-sphere system is now completely documented as far as the coherent density-fluctuation dynamics is concerned. A breakthrough was achieved by the application of the tandem Fabry–Pérot spectrometer. It allows the study of the evolution of structural relaxation within a four-orders-of-magnitude dynamical window extending from the Raman band for conventional condensed-matter dynamics down to 0.2 GHz. Similarly, it became possible very recently to explore by dielectric-loss spectroscopy the window extending from the far-infrared regime down to the low-frequency regime, which has been studied for a century. The results of this recent research have also been used to test MCT, and the outcome of this work will be reviewed in the following.

The essence of the MCT scenario for the evolution of structural relaxation is provided by asymptotic formulae derived for states near the glass transition singularities. The first problem for an assessment of MCT is therefore to find out whether or not the general theoretical results properly reflect the qualitative features of the experiments and the molecular dynamics simulations. The most objective description of such analyses can be communicated by quantitative comparisons of the data with the available formulae for the relevant asymptotic results. Hence I will proceed in this review by first citing some of the theoretical predictions, then explaining two figures from reports by authors who aimed to test the result under discussion, and finally I will consider related work obtained by other methods or for other systems. In reference [11] a summary of the basic MCT results can be found together with a list of the original publications on this subject, and therefore citations of papers dealing with theory will be omitted in the following.

2. The glass transition singularity

2.1. The form-factor anomaly

Within MCT the origin of the glassy relaxation is a fold bifurcation of the long-time limit f_q of the normalized density correlator $\phi_q(t) = \langle \rho_{\vec{q}}(t)^* \rho_{\vec{q}} \rangle / \langle |\rho_{\vec{q}}|^2 \rangle$, $q = |\vec{q}|$: $\phi_q(t \to \infty) = f_q$. This limit is zero for the liquid but positive for ideal glass states. It is called the glass form factor or the non-ergodicity parameter. It behaves discontinuously if a control parameter such as the packing fraction φ or temperature T passes some critical value φ_c or T_c respectively.

Thus f_q exhibits a singularity as a function of the distance $\epsilon = (\varphi - \varphi_c)/\varphi_c$ or $\epsilon = (T_c - T)/T_c$ for $\epsilon = 0$. A limit $f_q > 0$ is the Debye–Waller factor of the arrested disordered structure, since the normalized density-fluctuation spectrum reads

$$\phi_q''(\omega) = \pi f_q \delta(\omega) + \text{regular terms.}$$

In reality there are ergodicity-restoring processes for all choices of control parameters. They are referred to as hopping processes, and they are studied within the extended MCT which will not be discussed in detail in this article. For $\epsilon > 0$ the hopping processes change the ideal elastic spike $\pi f_q \delta(\omega)$ to a quasi-elastic peak. For $\epsilon < 0$ even the basic version of MCT predicts a quasi-elastic peak for the density spectrum $\phi_q''(\omega)$, whose width approaches zero in the limit $\epsilon \to 0$. The above-mentioned spectral peaks are the α-peaks of the MCT. The areas f_q of these peaks can be considered as effective Debye–Waller factors. For f_q, which can be measured by detecting the low-frequency spectrum $\phi_q''(\omega)$ or by determining the plateau of the $\phi_q(t)$-versus-log t curve, the prediction in the limit of vanishing hopping processes reads

$$f_q - f_q^c = \begin{cases} h_q \sqrt{\sigma/(1-\lambda)} + O_q(\sigma) & \sigma \geqslant 0 \quad (1a) \\ O_q'(\sigma) & \sigma < 0. \quad (1b) \end{cases}$$

Here $\sigma = C\epsilon$ is the separation parameter, $1/2 \leqslant \lambda < 1$ is the exponent parameter, $f_q^c > 0$ is called the critical form factor, the critical non-ergodicity parameter or the plateau, and $h_q > 0$ is called the critical amplitude. The introduction of C and λ in the results is a matter of convention, done in order to unify equation (1a) with formulae to be quoted in section 4. Equations (1) can be generalized to other normalized correlators $\phi_A(t) = \langle A^*(t)A\rangle/\langle|A|^2\rangle$ referring to variables A which couple to density fluctuations. One has to replace f_q^c and h_q by the A-specific amplitudes f_A^c and h_A respectively, where $0 < f_A^c < 1$ and $h_A > 0$. Also the corrections $O_A(\sigma)$ and $O_A'(\sigma)$ depend on the variable A, i.e. the ranges of validity of the specified leading-order results, $f_A - f_A^c \propto \sqrt{\epsilon}$ for $\epsilon > 0$ and $f_A = f_A^c$ for $\epsilon < 0$, depend on the variable under consideration.

For representative values q the predicted $\sqrt{\epsilon}$ anomaly relates to effects of the order of 10%. Typical experimental uncertainties render it difficult to identify the effect and to distinguish it from, e.g., a kink in the f_A-versus-T graph. Because of the change of the ideal spike to a quasi-elastic peak there is the additional problem of separating the peak from other contributions to the spectrum. Missing parts may introduce an artificial drop of the f_A-versus-T curve which

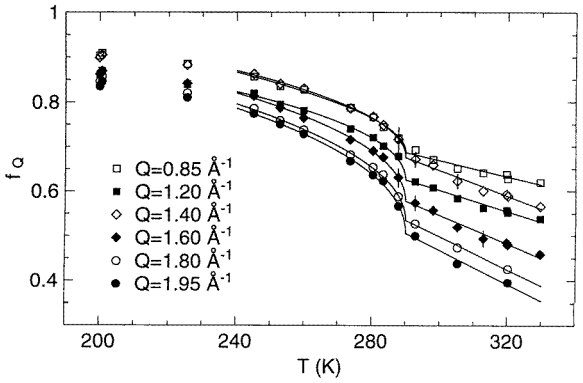

Figure 1. Effective Debye–Waller factors f_Q of OTP as functions of the temperature T measured for various wave-vectors Q by coherent neutron scattering spectroscopy. The curves indicate fits to equations (1) leading to a critical temperature $T_c \approx 290$ K. Based on figure 6 of reference [15].

overwhelms the searched-for cusp [12–14]. Even though the anomaly, equation (1a), refers to a $T < T_c$ property, one should therefore analyse the α-peak area also for $T > T_c$ in order to provide the base-line, equation (1b), for the anomaly.

Extensive neutron scattering studies for the van der Waals system orthoterphenyl (OTP, $T_g \approx 243$ K, $T_m = 329$ K) identified the square-root anomaly for the coherent and incoherent scattering cross sections with $T_c \approx 290$ K [5]. Figure 1 reproduces recent results for f_q obtained with neutron spin–echo and backward-scattering spectrometers [15]. The data relate to wave-vectors of the order of 1 Å^{-1}, i.e. they test fluctuations with wavelengths of the order of the interparticle distances.

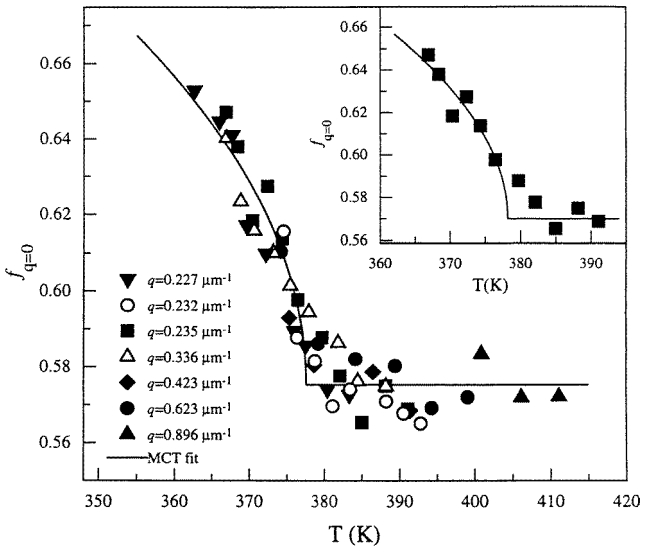

Figure 2. The effective Debye–Waller factor for wave-vector $q = 0$ of CKN as a function of the temperature T determined by impulsive stimulated light scattering spectroscopy. The results for $f_{q=0}$ are calculated from the generalized hydrodynamics formula for the scattering law for wave-vectors q. The inset shows results measured for $q = 0.235\ \mu\text{m}^{-1}$; the main part shows the combined results for all wave-vectors q studied. The curves are fits to equations (1) yielding a crossover temperature $T_c = 378 \pm 2$ K. Reproduced from reference [16].

The elastic modulus can be measured by impulsive stimulated scattering of light, thereby testing density fluctuations for macroscopic wavelengths. The anomaly for the modulus, measured by scattering from fluctuations of different wave-vectors q, can be converted to one of $f_{q=0}$. Figure 2 shows results obtained by this technique for the molten mixed salt $0.4\,Ca(NO_3)_2\,0.6\,KNO_3$ (CKN, $T_g \approx 333$ K, $T_m \approx 483$ K) [16]. These measurements identify the critical temperature $T_c = 378 \pm 2$ K. Notice that the anomalous Debye–Waller-factor drop, documented in figure 2 for the interval between $T_c - 15$ K and T_c, is only 13%. A small anomaly near the cited T_c has also been detected for an effective mean squared particle displacement of CKN by means of coherent neutron scattering spectroscopy [17]. The dielectric modulus of CKN exhibits a drop of about 20% consistent with the result of figure 2 [18].

For the van der Waals liquid Salol ($T_g \approx 218$ K, $T_m = 315$ K) the $\sqrt{\epsilon}$ anomaly was detected by incoherent neutron scattering spectroscopy [19] yielding $T_c = 263 \pm 7$ K. This value of the critical temperature is consistent with the result obtained by impulsive stimulated light scattering spectroscopy which identified a $\sqrt{\epsilon}$ anomaly of about 30% [20]. The same technique

was used also to identify the cusp anomaly for *n*-butylbenzene with $T_c \approx 150$ K [21]. Neutron scattering spectroscopy identified an f_q-anomaly for the van der Waals liquid propylene carbonate (PC, $T_g \approx 160$ K, $T_m = 218$ K) indicating $T_c = 190 \pm 20$ K [22].

Density correlators $\phi_q(t)$ have been determined for a set of wave-vectors by molecular dynamics studies for a binary mixture of Lennard-Jones particles $A_{50}B_{50}$ [23] and also for a three-site model for OTP [24]. The structural-relaxation parts have been fitted to the stretched exponential $f_q \exp -(t/\tau_q)^{\beta_q}$ in order to determine the effective Debye–Waller factor f_q. The results have been interpreted consistently with equation (1) and allowed the authors to estimate critical temperatures T_c. It was checked for the OTP model that the pair correlation functions, the structure factors, the density and the energy do not show any anomaly for T near T_c. The expected typical quenching anomalies were shown to occur at a temperature T_g below T_c [25]. Nevertheless, some reservation concerning the reported f_q is needed, since it is unclear whether the $T \leqslant T_c$ results in references [23, 24] are representative for properly equilibrated samples.

2.2. The position of the singularity

For some systems the MCT equations have been solved completely, thereby producing numerical values for f_q^c, h_q, λ, C from first principles. The simplest example is the hard-sphere system (HSS). It can be prepared for experimental studies as a colloidal suspension, and its density correlators $\phi_q(t)$, in particular the long-time limits f_q, can be determined by photon-correlation spectroscopy [26]. The predicted critical packing fraction $\varphi_c^{\mathrm{MCT}} = 0.525$ is somewhat smaller than the value measured for the transition from an ergodic liquid to a non-ergodic solid, $\varphi_c^{\mathrm{exp}} = 0.578 \pm 0.004$ [27].

Molecular dynamics studies for a carefully equilibrated binary Lennard-Jones mixture $A_{80}B_{20}$ (LJM) have been used for an extensive documentation of glassy dynamics and for tests of MCT [28–30]. For the states studied the structure is ruled by the $1/r^{12}$ repulsive part of the interaction potential and therefore the relevant control parameter for this system is $\Gamma \propto \varphi/(k_B T)^{1/4}$. For this system the MCT results for the numbers in equation (1) have been

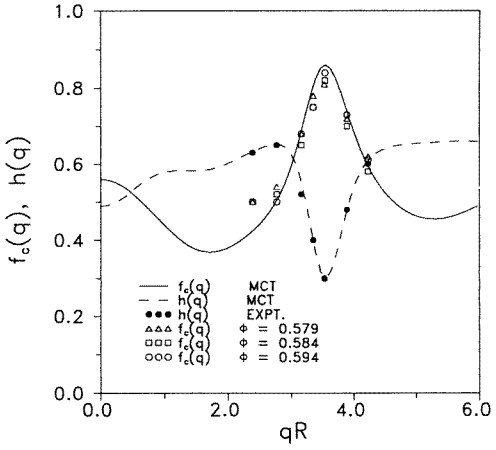

Figure 3. The critical Debye–Waller factor $f_q^c = f_c(q)$ (open symbols) and critical amplitude $h_q = h(q)$ (dots) as functions of the wave-vector q determined for a hard-sphere-colloidal glass by photon-correlation spectroscopy in comparison with the MCT predictions (curves) for the HSS. R denotes the particle radius and the main peak of the structure factor is located near $qR = 3.5$ Reproduced from reference [32].

evaluated in reference [31]. It was found again that MCT overestimates the trend to structural arrest and the discrepancy between calculated and measured critical couplings Γ_c is about 20%. This error transforms to a large discrepancy for the dimensionless critical temperatures $T_c^{\mathrm{MCT}} = 0.922$ versus $T_c^{\mathrm{exp}} = 0.435$. It is a notoriously difficult problem to accurately calculate from first principles a transition temperature for a condensed-matter system, and MCT calculations do not provide exceptions.

2.3. The glass form factors

The critical Debye–Waller factor f_q^c and the critical amplitude h_q have been measured for the HSS by analysing the long-time limit f_q of the density correlators for the above-mentioned colloid glass. Figure 3 reproduces some results [32]. Notice that there is no fit parameter involved in the comparison between the data and the MCT prediction for f_q^c. The data analysis in reference [32] in addition confirms the $\sqrt{\epsilon}$ decrease of f_q upon decreasing φ towards φ_c. The critical form factor f_q^c can also be deduced from liquid-state data by studying α-relaxation or β-relaxation scaling, as will be discussed below. Both methods have been applied in hard-sphere-colloid studies [33], corroborating and extending figure 3.

Unfortunately, molecular dynamics studies for the equilibrated states with $T \leqslant T_c$ have so far not been published. In non-equilibrated states, aging effects lead to a dynamics which is different from the one studied in MCT, and typical MCT features may be masked [34, 35]. For the cited LJM the symmetric two-by-two matrix of critical Debye–Waller factors f_q^c (the long-time limits of the normalized coherent scattering functions $\phi_q(t)$) and the two critical Lamb–Mössbauer factors f_q^{sc} (the long-time limits of the incoherent scattering functions $\phi_q^s(t)$) have been determined via equation (1*b*) from α-process studies of the equilibrated liquid. Figure 4 shows the findings for an f_q^c and an f_q^{sc} [36] in comparison with the MCT predictions from reference [31]. I will discuss below in connection with figure 15 how to determine from simulation data the Fourier back-transformation $H(r)$ of $S_q h_q$. Thereby one can obtain information equivalent to the knowledge of the critical amplitude h_q. It is shown in reference [31] that MCT accounts reasonably for the $H(r)$ data of the LJM.

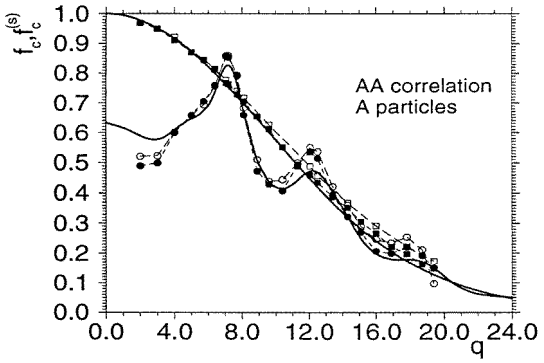

Figure 4. The critical form factor f_q^c (circles) and critical form factor for tagged-particle motion f_q^{sc} (squares) as functions of the wave-vector q deduced from fits of the von Schweidler law to the α-relaxation decay curves obtained by molecular dynamics simulations for a LJM. The broken lines are guides to the eye connecting the data points. The full curves are MCT results obtained for this system in reference [31]. The unit of length is chosen such that the structure factor peak is located near 7.3. The open symbols are results of simulations for a Newtonian dynamics and the filled ones for a stochastic dynamics. Reproduced from reference [36].

3. The two time fractals

The stretching of $\phi_q(t)$-versus-log t curves over large time windows or of the corresponding $\chi_q''(\omega)$-versus-log ω curves for the susceptibility spectra over huge frequency intervals is an outstanding feature of glassy dynamics. The MCT bifurcation dynamics exhibits this feature and the underlying mathematical essence of it is the appearance of two time fractals, i.e. power laws specified by non-integer exponents for the variation of the correlators $\phi_q(t)$ with time t. One fractal deals with the decay following the transient towards the plateau f_q^c and the other with the decay of the liquid correlators below this plateau.

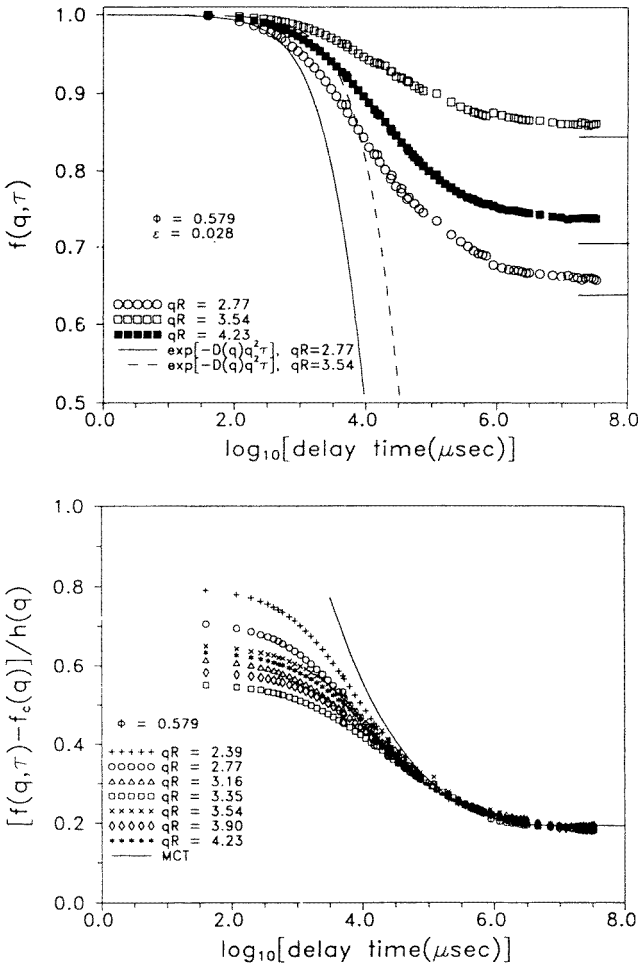

Figure 5. Density correlators $\phi_q(t) = f(q,\tau)$ (upper panel) and rescaled correlators $\hat{\phi}_q(t) = (\phi_q(t) - f_q^c)/h_q$ (lower panel) as functions of $\log_{10}(t)$, $t = \tau$, measured by photon-correlation spectroscopy for a hard-sphere-colloidal glass. The main peak of the structure factor S_q is located near $qR = 3.5$, where R denotes the particle radius. The upper panel exhibits as curves two exponential decay functions matched to the short-time diffusional asymptote. The full curve in the lower panel is the leading-order MCT result for the β-regime $\sqrt{|\sigma|}g_+(t/t_\sigma)$; the scales $|\sigma|$ and t_σ are fitted and the master function g_+ is the MCT result for the HSS. Reproduced from reference [32].

3.1. The critical decay law

The long-time decay process of the correlators at the critical point, called critical decay, is specified by an anomalous exponent a, $0 < a \leqslant a_{\max} = 0.395\ldots$, called the critical exponent. It is determined by the system-dependent exponent parameter λ as the solution of the equation $\Gamma(1-a)^2/\Gamma(1-2a) = \lambda$:

$$\phi_q(\hat{t}t_0) - f_q^c = h_q \hat{t}^{-a} + O_q^a(\hat{t}^{-2a}). \tag{2a}$$

Here f_q^c and h_q are the critical Debye–Waller factor and the critical amplitude respectively from equation (1a). Furthermore there enters a timescale t_0, determined by the transient, and $\hat{t} = t/t_0$ denotes a rescaled time. Correlators for other variables A which couple to the densities, such as the dipole moment, obey the same law; only f_q^c, h_q have to be replaced by the A-specific amplitudes f_A^c, h_A mentioned above, but a and t_0 remain unchanged.

The upper panel of figure 5 [32] reproduces density correlators for the cited hard-sphere-colloid glass for a packing fraction close to the critical one. Two exponential curves have been added to match the short-time diffusion-law asymptote. They indicate the normal-liquid dynamics. The data exhibit a stretched decay towards the long-time limit $f_q > f_q^c$ for times outside the transient regime, i.e. for $t \geqslant 10^3$ μs. For $qR = 2.77$ the anomalous dynamics relates to the decrease of $\phi_q(t)$ from 0.95 to about 0.65, and this decay is stretched over more than three orders of magnitude of time increase, before the long-time limit is reached within the error bars at about $10^{6.5}$ μs. The decay from 0.95 to 0.85 relates to the crossover from the transient to structural relaxation. The correlators follow the leading-order critical decay law

$$\hat{\phi}_q(t) = (\phi_q(t) - f_q^c)/h_q \propto 1/\hat{t}^a$$

only for a time interval of half a decade before they embark on the crossover for $t > 10^5$ μs to the limit f_q. So, the data shown demonstrate an anomalous decay process as predicted by MCT.

The critical law is equivalent to an enhancement of the fluctuation spectrum for $\omega t_0 \ll 1$ above a frequency-independent white-noise background according to the power law $\phi''(\omega) \propto 1/\omega^{1-a}$. This fluctuation spectrum corresponds to a sublinear susceptibility spectrum $\chi''(\omega) \propto (\omega t_0)^a$. Even though $\chi''(\omega)$ decreases with decreasing ω, it is enhanced above a regular susceptibility spectrum, $\chi''(\omega) \propto \omega$, caused by a white-noise background $\phi''(\omega) =$ constant. Figure 6 [37] demonstrates this behaviour for the 361 K dielectric-loss spectrum of the molten mixed salt $0.4\,Ca(NO_3)_2\,0.6\,RbNO_3$ (CRN). The data follow the power law for an exponent $a = 0.20$ over a three-decade window. A regular-background spectrum is indicated in the figure by the dotted line labelled $s = 1$. For $\omega/2\pi = \nu = 1$ GHz the measured spectrum is enhanced by more than a factor of 100 relative to the estimated regular contribution.

There are several reasons for which a demonstration of the pure $\hat{t}^{-a}$-law is the exception rather than the rule. To identify the power law, the time $t = t_0\hat{t}$ has to be chosen so large, or the frequency so small, that the correction term

$$O_A^a(\hat{t}^{-2a}) = \hat{h}_A \hat{t}^{-2a} + O(\hat{t}^{-3a}) \tag{2b}$$

can be neglected. Moreover one needs to choose t large because of the requirement that all transient effects must have disappeared. Not only can oscillations mask the critical law, but also they can produce crossover spectra $\chi''(\omega) \propto \omega^{a_{\text{eff}}}$, where the fit exponent a_{eff} is unrelated to a. On the other hand, one cannot choose t or $1/\omega$ arbitrarily large. First there is the signal-to-noise problem for the measurement of the small difference $\phi_q(t) - f_q^c$ or of the small intensity $\chi''(\omega)$ relative to the large nearby α-peak. Second, for $\sigma < 0$ there is the crossover to the α-process for large times or small frequencies as demonstrated for the $T = 381$ K results in figure 6. Similarly, for $\sigma > 0$ there is the crossover from the $1/\hat{t}^a$ decay to arrest at the

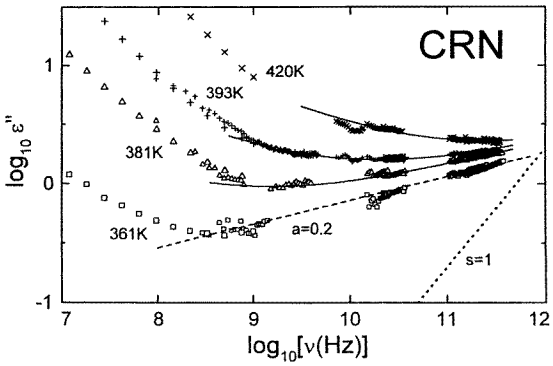

Figure 6. A double-logarithmic representation of the dielectric-loss spectrum ϵ'' of CRN as a function of frequency $\nu = \omega/2\pi$ for four temperatures. The dashed straight line shows the power law $\epsilon''(\omega) \propto \omega^a$, $a = 0.20$, and the dotted line shows an estimate of a white-noise-background spectrum $\epsilon''(\omega) \propto \omega^s$, $s = 1$. The full curves show the β-relaxation scaling law $\epsilon'' \propto \sqrt{|\sigma|}\hat{\chi}_-(\omega t_\sigma)$ with scales $\sqrt{|\sigma|}$ and t_σ fitted for each temperature. Here the interpolation formula $\hat{\chi}_-(\hat{\omega}) \propto [b\hat{\omega}^a + a\hat{\omega}^{-b}]$ is used where $a = 0.20$ and $b = 0.28$ are the exponents corresponding to the exponent parameter $\lambda = 0.91$. Reproduced from reference [37].

long-time limit f_q, as demonstrated in figure 5. The description of these crossovers from the critical decay to the α-process or to arrest respectively is a major subject of MCT, and the critical law manifests itself most clearly in this crossover feature. This is demonstrated for $\sigma > 0$ by the full curve in the lower panel of figure 5 and by the full curves in figure 6 as will be discussed in section 4.

3.2. The von Schweidler law

For the correlator decay of the liquid from the plateau f_q^c towards zero, i.e. for the start of the α-process, another power law is obtained, called von Schweidler's law:

$$\phi_q(\tilde{t}\tau) - f_q^c = -h_q\tilde{t}^b + O_q^b(\tilde{t}^{2b}). \tag{3a}$$

Here τ is the control-parameter-sensitive α-process timescale and $\tilde{t} = t/\tau$ denotes a rescaled time. The anomalous exponent b is also determined by the exponent parameter λ via $\Gamma(1+b)^2/\Gamma(1+2b) = \lambda$, $0 < b \leqslant 1$. The amplitudes f_q, h_q are the same as in equations (1a), (2a). The correction amplitude $\tilde{h}_q$ in the expression

$$O_q^b(\tilde{t}^{2b}) = \tilde{h}_q\tilde{t}^{2b} + \mathrm{O}(\tilde{t}^{3b}) \tag{3b}$$

is related to the corresponding amplitude in equation (2b): $\tilde{h}_q = \hat{h}_q + \Delta \cdot h_q$. Here Δ is a q-independent constant. The equations are generalized to other correlators $\phi_A(t)$ as before: one has to replace $f_q^c, h_q, \tilde{h}_q$ by $f_A^c, h_A, \tilde{h}_A$, respectively, but the scale τ and von Schweidler's exponent b remain unchanged.

Molecular dynamics simulations have been performed recently for a liquid of linear molecules, where the interaction was modelled by a two-site Lennard-Jones potential. The intention was to examine structural relaxation for the translational and rotational degrees of freedom and to test the applicability of the universal MCT results [38–40]. Figure 7 reproduces results of this work for the centre-of-mass density-fluctuation correlator for a tagged molecule for various temperatures as a function of the rescaled time t/τ. The smooth full curve exhibits a fit to the data of equations (3), using f_q^c, h_q, and $\tilde{h}_q$ as adjustable parameters. The fit with

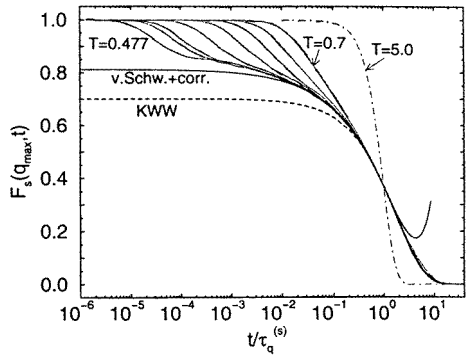

Figure 7. Tagged-particle density correlators ϕ_q^s for a wave-vector q at the position of the main peak of the structure factor as functions of the rescaled times t/τ. The data were obtained by molecular dynamics simulations for a liquid of diatomic molecules for dimensionless temperatures $T = 0.477$, 0.489, 0.500, 0.520, 0.549, 0.588, 0.632, 0.70, 5.0 (from left to right). The scale $\tau = \tau_q^s$ is chosen for each T such that the long-time parts of the correlators coincide. The smooth full curve is a fit to the von Schweidler asymptote $\phi_q(t) = f_q^c - h_q(t/\tau)^b + \tilde{h}_q(t/\tau)^{2b}$, $b = 0.54$. The dashed curve is a fit to the stretched exponential $\phi_q(t) = 0.7\exp -(t/\tau)^{0.78}$. Reproduced from reference [39].

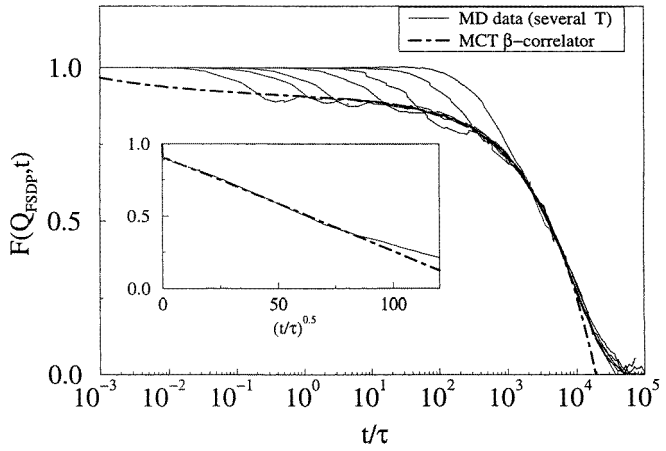

Figure 8. Density correlators $\phi_q(t) = F(Q,t)$ for a wave-vector $Q = 18\ \mathrm{nm}^{-1}$ near the position of the structure factor peak $Q = Q_{\mathrm{FSDP}}$ as functions of the rescaled time t/τ obtained by molecular dynamics simulations for a model of water. The α-relaxation time τ is defined by $\phi_q(\tau) = 1/\mathrm{e}$. The temperatures are from left to right 207, 210, 215, 225, 238, 258, 285 K. The dashed–dotted curve is the MCT leading-order β-relaxation result $f_q^c + h_q c_\sigma g_-(t/t_\sigma)$; the master function g_- is evaluated for the exponent parameter $\lambda = 0.79$ yielding a von Schweidler exponent $b = 0.50$, and f_q^c, $h_q c_\sigma$, t_σ are adjusted such that the data for 207 K are fitted for intermediate times. The inset is a rectification diagram where von Schweidler's law appears as the dashed–dotted straight line; it accounts for the 207 K data, which are shown as the full curve, for a dynamical window larger than two decades. Reproduced from reference [41].

$b = 0.54$ describes the decay from 0.75 to 0.25 perfectly. A test of equation (3*a*) is more suggestive and independent of the fit quantity f_q^c, if the correlator is rectified, i.e., if it is plotted as a function of t^b [28]. The inset of figure 8 shows such a plot with $b = 0.50$ for a density correlator obtained by molecular dynamics simulations for a model of water [41].

This result is one example of a series of findings [41–46] indicating that the slow dynamics of supercooled water is caused by a glass transition singularity at T_c around -50 °C. The quoted simulations were done for a rigid-point-charge model for the water molecules. The model reproduces the major features of the equation of state qualitatively but not quantitatively. Therefore one has to be cautious when one reaches conclusions on the properties of real water on the basis of simulation results.

From the analysis of depolarized light scattering spectra of Salol, measured within the GHz window, a von Schweidler exponent $b = 0.64 \pm 0.08$ was determined [47]. This value is corroborated by the result $b = 0.66 \pm 0.06$ obtained by fits of the von Schweidler law to the dynamic susceptibility curves $\chi(t) = -\mathrm{d}\phi(t)/\mathrm{d}t$ measured for Salol within the ps window in time-resolved optical Kerr-effect studies [48]. The high-frequency α-peak wing measured for the acoustic modulus of glassy LiCl in H_2O by impulsive stimulated light scattering could be fitted well over a window larger than three decades by von Schweidler's law with the value $b = 0.28$ [49]. The quoted examples confirm the MCT prediction that the anomalous exponent b is not universal but system specific.

Von Schweidler's law is a subtle asymptotic result of MCT and its experimental testing is complicated by the standard stumbling block: one does not *a priori* know its range of validity. One must not choose $t = \tilde{t}\tau$ too small, since for decreasing times $\phi(t)$ increases above f_q^c and merges with the critical decay law. Including erroneously such crossover parts into a fit to equation (3*a*) would lead to an underestimation of b and an overestimation of f_q^c. On the other hand, if $\tilde{t}$ is too large, the correction term from equation (3*b*) takes over. The near at hand fit criterion 'the larger the fit interval the better' has no justification. There is the danger that parts of the correction term are absorbed in the leading $h_q\tilde{t}^b$-term by choosing an incorrect fit exponent b or incorrect fit amplitudes f_q^c, h_q. This might lead to effective exponents depending on the wave-vector or, more generally, on the probing variable A. Suppose a whole set of correlators is available. Then one can use equations (3*a*), (3*b*) together and optimize the fit for all correlators simultaneously by varying h_q and $\tilde{h}_q$, but constraining b to a common number for all fit functions. The efficiency of this procedure, using density and tagged-particle-density correlators for a large set of wave-vectors q, was demonstrated for the analysis of the simulation results for water [44, 45]. The value $b = 0.50$, which was cited in connection with figure 8, resulted from such extensive data analysis. Similarly, it was shown that the correlators for translational as well as rotational variables for the model liquid of linear molecules could be interpreted with a common value $b = 0.54 \pm 0.05$, i.e. $\lambda = 0.76 \pm 0.03$. The exception to this demonstration of von Schweidler's law are all correlators dealing with rotation variables referring to the angular momentum index $\ell = 1$ [39, 40]. It seems that the molecule's dipole dynamics for the specified model is coupled so weakly to that of the density fluctuations that the asymptotic laws are not valid for the value of $T - T_c$ studied.

4. Dynamics within the first-scaling-law regime

4.1. β-relaxation scaling

The dynamics in a window where $\delta\phi_q(t) = \phi_q(t) - f_q^c$ is small is referred to as β-relaxation and there one finds

$$\delta\phi_q(t) = h_q G(t) + O_q(|\sigma|, \sqrt{|\sigma|}G(t), G(t)^2).$$

The result can be generalized to correlators for other variables A as discussed above, where A-specific amplitudes f_A^c and h_A enter. Thus the leading-order result reads

$$\phi_A(t) - f_A^c = h_A G(t). \tag{4a}$$

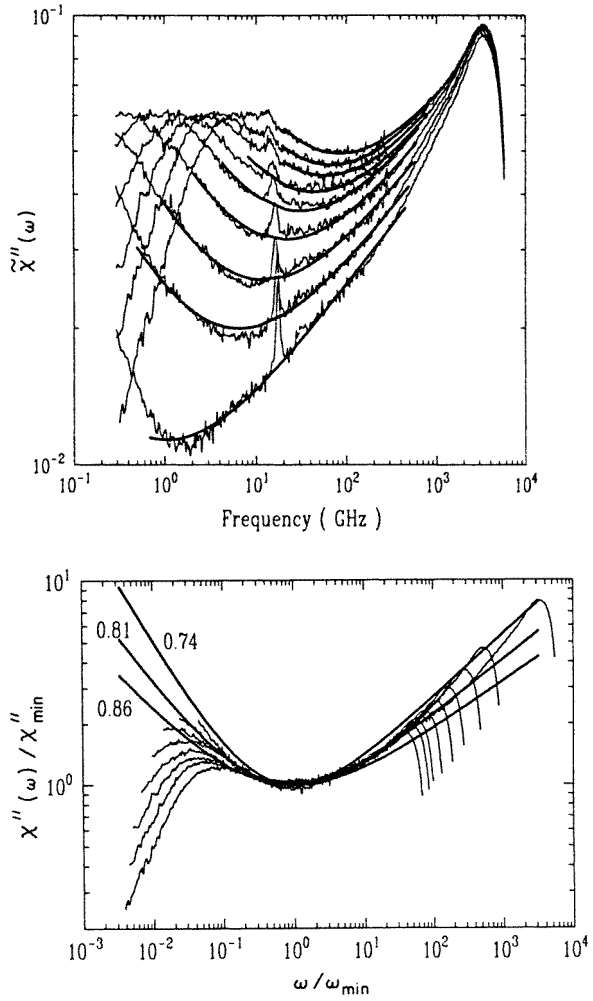

Figure 9. Double-logarithmic plots of the susceptibility spectra $\chi''(\omega)$ as functions of the frequency $\omega/2\pi$ measured by depolarized light scattering for CKN. The top panel shows the results for the temperatures (from top to bottom) 195, 180, 170, 160, 150, 140, 130, 120, and 110 °C. The full curves are the approximations to the master spectra $\hat{\chi}_-(\hat{\omega}) \propto [b\hat{\omega}^a + a\hat{\omega}^{-b}]$ translated such that the spectra are matched near the minimum. The anomalous exponents $a = 0.27$ and $b = 0.46$ correspond to the exponent parameter $\lambda = 0.81$. The bottom panel exhibits the spectra translated such that the minimum positions $\omega_{\min}$ and minimum intensities $\chi''_{\min}$ coincide. The full curves are the master spectra for $\lambda = 0.86$, 0.81, and 0.74. Reproduced from reference [50].

This formula is called the factorization theorem. It is equivalent to the formula for the susceptibility spectrum

$$\chi''_A(\omega) = h_A \chi''(\omega). \tag{4b}$$

Here $\chi''(\omega) = \omega G''(\omega)$ with $G''(\omega)$ denoting the Fourier-cosine transform of $G(t)$. The function G, called the β-correlator, depends on t/t_0 and σ, where the timescale t_0 is the one from equations (2), and σ is the separation parameter from equations (1). The power law $G(t) = (t_0/t)^a$ holds for $\sigma = 0$, so equation (2a) is reproduced, and for $\sigma \neq 0$ one gets

$$G(t) = c_\sigma g_\pm(t/t_\sigma) \qquad \sigma \gtrless 0. \tag{5a}$$

This is equivalent to the corresponding scaling law for the susceptibility spectrum: $\chi''(\omega) = \Gamma(1-a)\sin(\pi a/2)(\omega t_0)^a$ for $\sigma = 0$ and

$$\chi''(\omega) = c_\sigma \hat{\chi}_\pm(\omega t_\sigma) \qquad \sigma \gtrless 0 \tag{5b}$$

with $\hat{\chi}_\pm(\hat{\omega}) = \hat{\omega}\hat{g}''_\pm(\hat{\omega})$ and $\hat{g}''_\pm(\hat{\omega})$ denoting the Fourier-cosine transform of $g_\pm(\hat{t})$. The control-parameter-independent master functions $g_\pm(\hat{t})$ and $\hat{\chi}_\pm(\hat{\omega})$ are determined solely by the exponent parameter λ. The sensitive dependence of $\phi_A(t)$ on control parameters is described by the two scales c_σ and t_σ, whose σ-dependence will be discussed below.

The β-relaxation scaling is tested most conveniently by studying $\log \chi''(\omega)$-versus-$\log \omega$ plots. According to equations (4*b*), (5*b*) the spectral shape is given by the $\log \hat{\chi}_\pm(\hat{\omega})$-versus-$\log \hat{\omega}$ graph, and spectra for different control parameters are related by mere translations of this curve. Figure 9 demonstrates this law for depolarized light scattering spectra measured for CKN for $T > T_c$; the data combine Raman spectrometer and tandem Fabry–Pérot spectrometer results. To obtain relaxation spectra which are not disturbed by hydrodynamic shear excitations the measurements were done for backward scattering. This experiment was the first which displayed the evolution of structural-relaxation spectra within the GHz window upon cooling a glass-forming liquid [50]. The top panel shows also the $\lambda = 0.81$ master function $\hat{\chi}_-$, translated for each T such that it interpolates the spectral minima. The figure demonstrates that the theoretical $\hat{\chi}_-$ accounts for the 120 °C data within a window of nearly three orders of magnitude. The fits start to be valid for frequencies just below the microscopic-excitation band due to oscillations which extends down to about 0.4 THz. The bottom panel shows that a translation of the spectra onto the master curve for $\lambda = 0.81$ is possible within a window of rescaled frequencies $\omega/\omega_{\min}$ which is larger for smaller $|T - T_c|$. Other values for λ differing by up to ± 0.05 could be tolerated for an alternative fit. The interpretation of the light scattering spectra was corroborated by the one given for the dielectric function [37]. The loss spectra of CKN exhibit a minimum for $T \leqslant 144$ °C. The real and imaginary parts of the dielectric function for frequencies below 315 GHz were described by the scaling law and fitted with the master functions for $\lambda = 0.76$. For $T = 106$ °C the fit describes the spectrum for a four-decade frequency window.

Figure 10 shows a test of the scaling law in the time domain. The data refer to density correlators measured with photon-correlation spectroscopy for various packing fractions φ for colloidal suspensions of polysterene-micronetwork spheres [51]. The full curves exhibit the formulae (4*a*), (5*a*) for $f_A = 0.89$, $\lambda = 0.88$. For each φ the two scales $c_\sigma h_A$ and t_σ were fitted. These fits of the scales account for the observed strong variation of the dynamics, reflected by an increase of the time τ, where $\phi_A(\tau) = 0.5$, of over more than four orders of magnitude. The master function $g_-(\hat{t})$ describes the decay of the correlator between 0.95 and 0.50, which for sample E extends over the huge time window of about seven orders of magnitude.

The most extensive test of the β-scaling predictions was carried out in the work on hard-sphere colloids [27, 32, 33]. For seven representative wave-vectors q the functions $\hat{\phi}_q(t) = (\phi_q(t) - f_q^c)/h_q$ were shown to be given by $c_\sigma g_\pm(t/t_\sigma)$ for $\varphi > \varphi_c$ and $\varphi < \varphi_c$ respectively within the appropriate window, and for master functions $g_\pm$ referring to the value $\lambda = 0.77$ predicted for the HSS from first-principles calculations. The evaluation of this λ is based on the Verlet–Weiss approximation for the structure factor. It was checked that the largest change of λ, which might be tolerated for an alternative data analysis, is ± 0.05 [33]. The lower panel of figure 5 reproduces an example of this work. The full curve exhibits the scaling-law result $c_\sigma g_+(t/t_\sigma)$ for fitted values for the scales c_σ, t_σ. It describes the data for $\hat{\phi}_q(t)$ of the glass for a time interval of 2.5 decades for $t > 10^5$ μs.

The evolution of the enhanced susceptibility minimum on cooling was measured also for Salol by depolarized light scattering spectroscopy. A description by the β-relaxation scaling

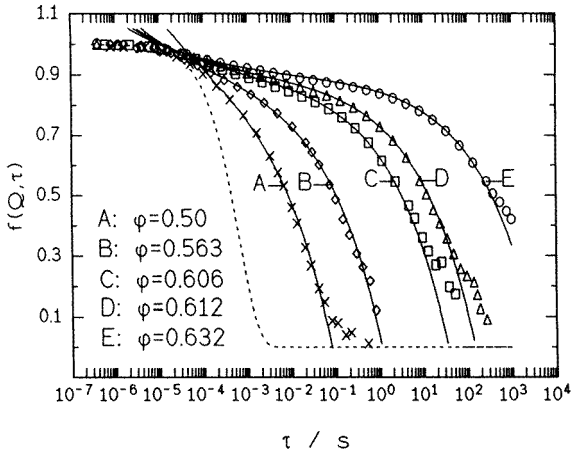

Figure 10. Density correlators $\phi_q(t) = f(Q,\tau)$ measured as functions of time $t = \tau$ by photon-correlation spectroscopy for five packing fractions φ for a colloidal suspension of polysterene-micronetwork spheres. The full curves are the scaling-law result $\phi_q(t) = f_q^c + h_q c_\sigma g_-(t/t_\sigma)$ with $f_q^c = 0.89$, a master function $g_-(\hat{t})$ calculated for the exponent parameter $\lambda = 0.88$, and the two scales $h_q c_\sigma$, t_σ fitted for each packing fraction. The dotted curve shows the transient dynamics $\exp -(t/t_{\rm mic})$ with $t_{\rm mic}$ matched to the short-time asymptote. Reproduced from reference [51].

law was shown to be possible for frequencies below 0.1 THz and it led to the determination of the exponent parameter $\lambda = 0.70 \pm 0.05$, implying the anomalous exponents $a = 0.33$ and $b = 0.64$ [47]. The spectral minimum of Salol was observed also by inelastic neutron scattering [52]. For temperatures near T_c the minimum frequency $\omega_{\rm min}$ was close to that reported for the light scattering data. For $T - T_c > 20$ K the minima became different, indicating that the corrections to the leading-order result, equation (5*b*), are different for the two probing variables A studied in the two cited experiments. The existence of the anomalous minimum between the α-peak and the far-infrared excitation band of Salol was shown for $T = 293$ K by dielectric-loss spectroscopy [53], but the frequency window studied was too small to allow for a quantitative analysis of the data.

Another van der Waals liquid, for which the depolarized light scattering spectra could be described by the β-scaling law for a frequency window of up to three orders of magnitude, is PC; $\lambda = 0.78 \pm 0.05$ was found [54]. This result was corroborated by dielectric-loss spectroscopy [55]. A transient hole-burning experiment was performed to measure a normalized decay curve $\phi_A(t)$, which describes the structural relaxation of the environment of an excited dye molecule soluted in PC. The formulae (4*a*), (5*a*) describe the data for a time window larger than two orders of magnitude, where the master function $g_-(\hat{t})$ was used for the same $\lambda = 0.78$ [56]. In this work a scaling-law analysis is also demonstrated for *n*-butylbenzene as solvent where $\lambda = 0.86$ was identified.

Raman-scattering spectra for m-tricresyl phosphate also exhibited a susceptibility minimum which is enhanced above an estimated white-noise background. It can be described for the large temperature variation range of 95 K by the scaling-law expression, equation (5*b*), with a master function $\hat{\chi}_-$ for $\lambda = 0.65$ [57]. It would be desirable to corroborate these results by the analysis of spectra extending to lower frequencies.

The depolarized light scattering spectra of toluene ($T_g \approx 118$ K, $T_m = 178$ K), measured with a tandem Fabry–Pérot spectrometer for frequencies between 1 and 200 GHz and for temperatures between 142 and 179 K, could be described well by the scaling law using a

master function for $\lambda = 0.73 \pm 0.03$. The same description was possible for spectra obtained by incoherent neutron scattering for frequencies above 35 GHz [58].

The high-frequency wing of the susceptibility minimum can be analysed by asymptotic MCT formulae only for such low frequencies that conventional condensed-matter vibrational spectra can be neglected. It was demonstrated that by application of up to 7.6 kbar pressure to isopropylbenzene ($T_g \approx 125$ K, $T_m = 177$ K) the spectral contributions due to oscillations are shifted to frequencies above 2 THz. Therefore a dynamical window of more than three orders of magnitude could be used for the scaling-law analysis of the spectral minimum which was measured by depolarized light scattering spectroscopy. The exponent parameter $\lambda = 0.80$ was determined and the timescale t_σ could be identified, where now the pressure was used as the control parameter [59]. Unfortunately, the spectra could not be calibrated, so the scale $h_A c_\sigma$ could not be determined.

Inelastic neutron scattering spectroscopy yields the convolution of the fluctuation spectrum $\phi_q''(\omega)$ with the instrument's resolution function. The latter can be eliminated in principle by Fourier deconvolution and thereby one obtains $\phi_q(t)$. By combining of results from two or three spectrometers, structural-relaxation results for OTP could be obtained by incoherent [60] and coherent [15] scattering for wave-vectors q between 0.8 Å^{-1} and 2.0 Å^{-1}. The data obey the scaling law $\phi_A - f_A^c = h_A c_\sigma g_-(t/t_\sigma)$ for a dynamical window larger than two orders of magnitude [15, 60, 61] for the common exponent parameter $\lambda = 0.77$. It is difficult to estimate the uncertainty of λ, but ± 0.05 is perhaps not too pessimistic. A β-scaling analysis consistent with the cited results has also been carried out using a pressure shift between 0.1 and 120 MPa as control parameter [62]. Comparing the changes of $\phi_q(t)$ due to variations with temperature and with pressure, it was found that the relevant control parameter is the quantity $\Gamma \propto \varphi/T^{1/4}$. One would expect such a result if the glassy dynamics was governed by the structure in a regime, which is dominated by a $1/r^{12}$ repulsive potential. A comprehensive MCT analysis of depolarized light scattering spectra, measured for the frequency window between 0.2 GHz and 3 THz, has also been done for OTP [63]. The microscopic-excitation band due to the transient dynamics extends down to about 0.2 THz for this system. The β-relaxation scaling analysis works well with $\lambda = 0.72$ for temperatures between 340 K and 300 K and it describes the 300 K spectrum around the susceptibility minimum for a window of 2.5 decades. The above-mentioned computer experiments for an OTP model [24, 25] detected the crossover from the α-relaxation process to the critical decay. This crossover could be described by equation (4*a*) for an incoherent density-fluctuation correlator and reorientational correlators for angular momentum index $\ell = 1$ and $\ell = 2$. Since the β-relaxation window identified is rather small and since the data exhibit a considerable noise, there has to be some reservation concerning the exponent parameter used, $\lambda = 0.56$, which is considerably smaller than the one found for OTP in laboratory experiments [64].

The above-mentioned scaling laws are asymptotic results for the dynamics near the critical point. This implies in particular that the interval for $\log t$ or $\log \omega$, where the law is valid, has to grow monotonically if $|\sigma|$ decreases. Figures 9 and 10 show examples of this phenomenon for decreasing T and increasing φ respectively. A demonstration of this manifestation of asymptotics is a crucial step in every analysis of the scaling-law predictions.

4.2. The β-relaxation scales

According to equation (5*b*) the intensity $\chi''_{\min}$ and position $\omega_{\min}$ of the susceptibility spectrum minimum are proportional to c_σ and $1/t_\sigma$ respectively. But signal-versus-noise problems make it difficult to read these numbers off directly from the data plots, as is obvious from figure 9. For the same reason it is difficult to deduce the scales directly from $\phi(t)$-versus-$\log t$ diagrams.

This could be done in principle by using the equations

$$\phi_q(t_-) = f_q^c \qquad t_- \propto t_\sigma \qquad f_q^c - \phi_q(2t_-) \propto c_\sigma .$$

It is more straightforward to obtain the scales as a by-product of the scaling-law verification. For example, the vertical and horizontal translations studied in the double-logarithmic plots in figure 9, needed to bring the master spectrum onto the data (top panel) or the data onto the master spectrum (bottom panel), are $\log c_\sigma$ and $\log t_\sigma$ respectively, up to some additive σ-independent constant. For the scales, power laws are predicted. The amplitude scale is the elementary square root, characterizing a fold bifurcation:

$$c_\sigma = \sqrt{|\sigma|}. \tag{6}$$

The timescale, called the first critical timescale or β-relaxation scale, is specified by an anomalous exponent $1/2a$ larger than 1.27:

$$t_\sigma = t_0/|\sigma|^{1/2a}. \tag{7}$$

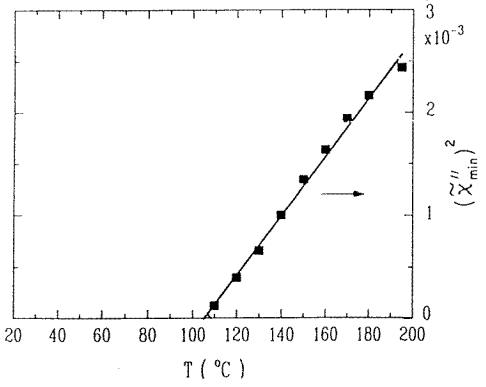

Figure 11. Squares of the spectral intensity of the susceptibility at the minimum, $\chi^2_{\min}$, versus the temperature, where $\chi_{\min}$ is obtained from the scaling-law analysis of the CKN depolarized light scattering data shown in figure 9. The line is a linear interpolation of the data points and its intersection with the abscissa yields the estimate of the crossover temperature $T_c \approx 105\,^\circ$C. Based on figure 7 of reference [50].

The $\sqrt{|\epsilon|}$ law for the amplitude scale is verified in figure 11 [50] for the light scattering spectra of CKN discussed in figure 9 by showing that the $(\chi''_{\min})^2$-versus-T diagram is a straight line: $c_\sigma^2 \propto |\sigma| \propto (T - T_c)$. This finding is corroborated by the results obtained by the analysis of dielectric-loss spectra of CKN, as shown by the top panel of figure 12 [37]. The intersections of the straight lines shown with the abscissa yield two estimates of T_c from the high-temperature side of this crossover temperature. The values are consistent with the one obtained from the low-temperature side by studying the Debye–Waller-factor anomaly, discussed above in connection with figure 2. Let us note that $g_+(\hat{t} \to \infty) = 1/\sqrt{1-\lambda}$, so equations (4$a$), (5$a$) yield $\phi_A(t) - f_A^c = h_A c_\sigma/\sqrt{1-\lambda}$ for $\sigma > 0$. Therefore, the $\sqrt{\sigma}$ expression in equation (1a) is an implication of equation (6) for $T < T_c$.

The increase of the timescale $\tau_\beta^- = 1/\omega_{\min}$ by nearly two orders of magnitude upon cooling, deduced in reference [50] from the scaling-law analysis of the CKN light scattering spectra in figure 9, is demonstrated by the squares in figure 13. The data are compatible with the predicted power law, equation (7), which is shown as a full curve. It is more informative to present the data as a rectification diagram, i.e. as a $1/(\tau_\beta^-)^{2a}$-versus-T plot. The validity of equation (7) is equivalent to the observation that the data can be interpolated linearly. In

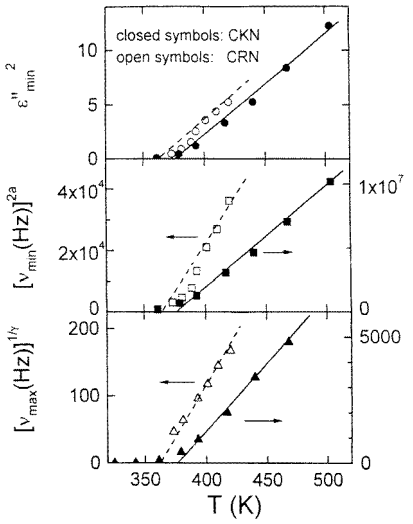

Figure 12. The temperature dependences of $\epsilon''^{2}_{\rm min}$, $\nu^{2a}_{\rm min}$, and $\nu^{1/\gamma}_{\rm max}$ determined for the molten salts CKN and CRN. Here $\epsilon''_{\rm min}$ and $\nu_{\rm min}$ denote the height and frequency of the minimum of the dielectric-loss spectra, and $\nu_{\rm max}$ is the α-peak frequency. The exponents a and γ are the ones obtained from the exponent parameters $\lambda = 0.76$ (CKN: $a = 0.30$, $\gamma = 2.6$) and $\lambda = 0.91$ (CRN: $a = 0.20$, $\gamma = 4.3$) used for the master functions for the scaling-law analysis of the spectral minima. The straight lines are linear interpolations of the data, and their intersection with the abscissa occurs for CKN near 375 K and for CRN between 360 K and 375 K. Reproduced from reference [37].

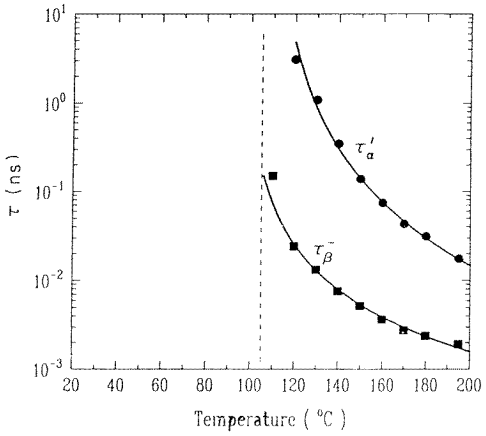

Figure 13. The temperature dependences of the scaling times τ^-_β and τ'_α for the β-relaxation minimum and the α-peak maximum respectively of the depolarized light scattering spectra measured for CKN. The scale $\tau^-_\beta = 1/\omega_{\rm min}$ was obtained by the scaling-law analysis discussed in connection with figure 9. The scale $\tau'_\alpha \propto \tau$ was obtained by verifying the second scaling law of MCT, equation (8*b*). The full curves show the MCT power laws $\tau^-_\beta \propto t_\sigma \propto |T - T_c|^{-1/2a}$, $\tau'_\alpha \propto \tau \propto |T - T_c|^{-\gamma}$, with $1/2a = 1.8$ and $\gamma = 2.9$, obtained from the exponent parameter $\lambda = 0.81$. Based on figure 16 of reference [50].

addition one gets from the intersection of the straight-line interpolation with the abscissa a value for the crossover temperature T_c, which thereby was found [50] to be consistent with the other measurements mentioned above. The middle panel of figure 12 corroborates the

findings, but now for dielectric-loss data for CKN [37]. Figure 12 also exhibits an analysis of the scales for the dielectric-loss spectra of CRN, based on the scaling-law fit shown in figure 6. Obviously, the results for CRN are less convincing than those reported for CKN in reference [37]. It is also puzzling that the two systems CKN and CRN, which are chemically so similar, should have such different exponent parameters as 0.76 and 0.91, respectively.

The scales deduced from the scaling-law analysis of depolarized light scattering spectra of Salol followed the pattern discussed above and provided two determinations of the critical temperature $T_c = 256 \pm 5$ K [47], a value consistent with the results of neutron scattering studies of the susceptibility minimum [52]. These determinations of T_c from the $T > T_c$ side led to somewhat smaller values than the determination from the $T < T_c$ side via a test of equation $(1a)$ by neutron scattering ($T_c \approx 260$ K) [19] and impulsive stimulated light scattering ($T_c = 266$ K) [20] experiments. Scaling-law analysis of the β-relaxation of PC studied by light scattering [54], transient hole-burning [56], and dielectric-loss [55] spectroscopy confirmed the validity of equations (6), (7) and provided a consistent estimate $T_c \approx 180$ K. The scales, which could be deduced from the above-cited studies of m-tricresyl phosphate [57] and isopropylbenzene [59] followed the MCT predictions. The same holds for the results found for the *n*-butylbenzene analysis [56], which provided an estimate of T_c which is about 10 K above the value derived from the Debye–Waller-factor anomaly [21]. The comprehensive tests of MCT by the analysis of depolarized light scattering spectra of OTP supported the predictions for the scales c_σ, t_σ for $T > T_c$ and led to $T_c \approx 290$ K [63]. This value is consistent with the above-mentioned analysis of the glass form-factor anomalies by incoherent [4, 5] and coherent [5, 15] neutron scattering spectroscopy. The successful test of the β-relaxation scaling for incoherent [60, 61] and coherent [15] neutron scattering of OTP led to scales c_σ and t_σ confirming equations (6), (7) and the cited T_c. The scaling-law analysis of the toluene spectra confirmed the predictions for the power-law variations of the scales and provided the estimate of the critical temperature $T_c = 143 \pm 3$ K [58].

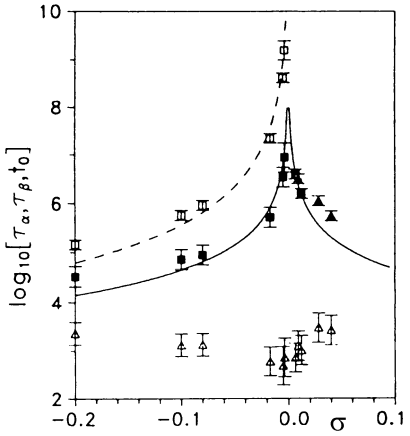

Figure 14. The scaling times $\tau_\alpha = \tau$ (open squares) obtained from the scaling-law analysis of the α-process and $\tau_\beta = t_\sigma$ (filled symbols) obtained from the β-relaxation scaling analysis for the density correlators measured by dynamic light scattering spectroscopy for colloidal suspensions of hard spheres as functions of the separation parameter $\sigma = C(\varphi - \varphi_c)/\varphi_c$. The full curves exhibit the first critical timescale $t_\sigma = t_0/|\sigma|^{1/2a}$, $1/2a = 1.7$, and the dashed curve shows the second critical timescale $\tau = t_0 B^{1/b}/|\sigma|^\gamma$, $\gamma = 2.6$, $b = 0.53$, $B = 1.01$, of the HSS. The open triangles denote the timescale t_0 from the transient dynamics used in the fits. Reproduced from reference [33].

The β-scaling analysis for the hard-sphere-colloidal liquid ($\sigma < 0$) and the glass ($\sigma > 0$) leads to scales confirming the MCT formulae [27, 32, 33]. This is demonstrated in figure 14 for the timescales by the comparison of the measured scaling times (full symbols) with the predicted result, equation (7) with $1/2a = 1.7$. Notice that MCT relates the master function $g_+(\hat{t})$ with $g_-(\hat{t})$ in equation (5*a*). This was accounted for in the scaling-law analysis. The fact that the data points in figure 14 indicate a symmetry of the cusp of the $1/t_\sigma$-versus-σ curve without adjusting the constants of proportionality provides support for the MCT relation between the slow bifurcation dynamics of the liquid and that of the glass.

The analysis of the β-relaxation of the colloidal suspension of polysterene-micronetwork spheres, discussed above in connection with figure 10 for $\varphi < \varphi_c$, is summarized in reference [65]; it shows full agreement with the MCT predictions. However, for $\varphi > \varphi_c$ MCT can account for the data only for a time window of less than two decades, because in this material there appears a new relaxation process of unknown origin for long times [66].

4.3. The factorization property

The factorization of $\phi_A(t) - f_A^c$ into a time-and-control-parameter-independent A-specific amplitude h_A and a function $G(t)$ of time t and separation parameter σ, which is shared by all probing variables A, equation (4*a*), has surprising implications. If applied to the particle density $n(\vec{r}, t)$ as a function of the position vector $\vec{r}$, it reads $\phi(r, t) - F(r) = H(r)G(t)$. Here $F(r), H(r)$ are the Fourier back-transformations of $S_q f_q^c$ and $S_q h_q$ respectively and $\phi(r, t) = \langle n(\vec{r}_1, t_1) n(\vec{r}_2 t_2)\rangle$ denotes the correlation function for densities; $\vec{r} = \vec{r}_1 - \vec{r}_2$, $t = t_1 - t_2$, $r = |\vec{r}|$. For the β-relaxation window it is therefore predicted that the variations of the densities in space are uncorrelated with those in time. A practical way to test this statement [8] is based on the rewriting of equation (4*a*) as

$$\Delta\phi(r, t) = \phi(r, t) - \phi(r, t') = H(r)[G(t) - G(t')].$$

Here t' is some time at the end of the β-relaxation window. The result to be checked is equivalent to the property that $\Delta\phi(r, t)/\Delta\phi(r', t) = H(r)/H(r')$ is time independent. The property has been verified for several correlators, obtained in the simulation work for a LJM [29], and figure 15 reproduces an example. The cited tests for the factorization hold for an intermediate-time window, which is larger than 2.5 orders of magnitude. Lest the result found be considered trivial, it should also be pointed out that it was demonstrated explicitly in reference [29] that the factorization holds neither for the short-time transient nor for the long-time part of the α-process.

The factorization of the wave-vector dependence and the time dependence of the function $\phi_q(t) - f_q^c$, measured for the hard-sphere colloid within the β-relaxation window, was demonstrated for a representative set of wave-vectors q around the position of the structure factor peak in references [27, 32, 33]. The lower panel of figure 5 exhibits an example for the glass state. The factorization holds for the 2.5-decade window $t > 10^5\ \mu$s. It does not hold for shorter times relating to transient dynamics and to the crossover to structural relaxation. Indeed, the initial part of the correlators is given by the law for diffusion $\phi(t) = \exp[-D(q)q^2 t]$, and this is a paradigm for hydrodynamically correlated propagation of density fluctuations in space and time. The initial part of the α-process, described by von Schweidler's law, also exhibits the factorization property; however, the final parts of the liquid correlators do not [33].

The verification that the intermediate-scattering functions of OTP for incoherent [60] and coherent [15] neutron scattering in the appropriate regime $|\phi_q(t) - f_q^c| \ll 1$ can be written as $\phi_q(t) - f_q^c = h_q G(t)$ with a common scaling function $g_-(\hat{t})$ according to equations (4*a*), (5*a*), and this for a representative set of wave-vectors between 0.8 Å^{-1} and 2 Å^{-1}, is a further

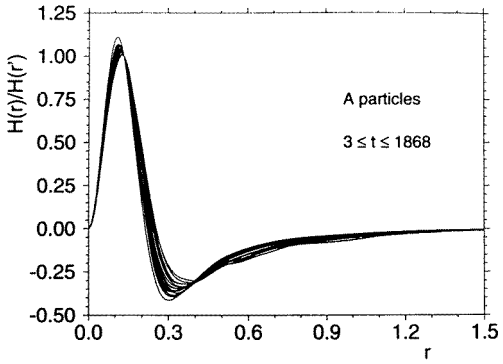

Figure 15. The ratios $\Delta\phi(r,t)/\Delta\phi(r',t')$ of the tagged-particle-density correlation function differences $\Delta\phi(r,t) = \phi(r,t) - \phi(r,t')$ as functions of the distance r obtained from molecular dynamics simulations for a LJM. The unit of length is chosen such that the peak of the pair correlation function $g(r)$ is located near 1. The time t' is chosen at the end of the β-relaxation window. The times t are spaced evenly on a logarithmic axis covering 2.8 decades. Validity of the factorization theorem $\phi(r,t) = F(r) + H(r)G(t)$ is equivalent to a coalescence of the ratios to the time-independent function $H(r)/H(r')$. Reproduced from reference [29].

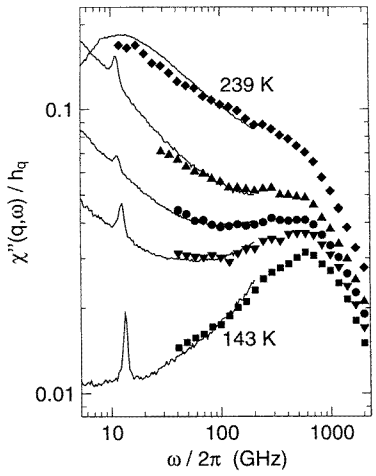

Figure 16. A double-logarithmic representation of susceptibility spectra $\chi_q''(\omega)/h_q$ of toluene as functions of the frequency $\nu = \omega/2\pi$ for temperatures $T = 143$, 159, 169, 191, 239 K (from bottom to top). The symbols show results obtained by incoherent neutron scattering spectroscopy for wave-vectors q between 0.5 Å^{-1} and 1.8 Å^{-1}. The curves are spectra obtained by depolarized light scattering. Reproduced from reference [58].

demonstration of the factorization property. The studies of glassy toluene [58] provided an explicit verification of equation (4*b*) which is shown in figure 16. The neutron scattering spectra in the β-relaxation window could be described for five wave-vectors between 0.5 Å^{-1} and 1.8 Å^{-1} by equation (4*b*), and in addition the same spectra $\chi''(\omega)$ accounted for the light scattering data. It should be added that the low-frequency parts of the α-processes, which are not reproduced in figure 16, do not exhibit the factorization property [58].

Another test of the factorization was carried out by comparing the light scattering spectra for CKN [50] with neutron spin–echo measurements of the density correlators [67]. It was

shown that the neutron scattering data could be described within the β-relaxation window by equation (4*a*). Here a constant f_A and a smoothly drifting h_A were chosen as the only fit parameters; $G(t)$ was the β-correlator obtained by back-transforming the susceptibility spectrum $\chi''(\omega)$ from the fit of light scattering data [50]. The fit was done within the extended MCT, which accounts also for the influence of thermally activated jump processes on the β-relaxation dynamics [68]. The interpretation of the neutron scattering data could be done even with a temperature-independent amplitude h_A if the contribution of the α-process was considered [69]. Unfortunately, the window accessible for the spin–echo spectrometer and the accuracy of the data are not sufficient to enable one to use the cited neutron scattering results as proof of the correctness of MCT, as was emphasized in reference [70]. Nevertheless it is support for the theory that a quantitative interpretation of a strongly temperature-dependent set of correlation functions for the stretched dynamics of CKN [67] can be given by choosing only two temperature-independent amplitudes f_A, h_A as fit parameters.

5. Dynamics within the second-scaling-law regime

5.1. α-relaxation scaling

The dynamics within the window, where the liquid correlators decay from the plateau f_q^c to zero, is referred to as α-relaxation. One gets the asymptotic expansion: $\phi_q(\tilde{t}\tau) = \tilde{\phi}_q(\tilde{t}) + O_{\tilde{t}}(\sigma)$, where the α-relaxation scale τ is normalized according to equation (3*a*): $\tilde{\phi}_q(\tilde{t} \to 0) = f_q^c - h_q\tilde{t}^b + \mathrm{O}(\tilde{t}^{2b})$. The result can be generalized to correlators of other variables A to give, to leading order,

$$\phi_A(t) = \tilde{\phi}_A(t/\tau). \tag{8a}$$

This is equivalent to the formula for the susceptibility

$$\chi_A(\omega) = \tilde{\chi}_A(\omega\tau). \tag{8b}$$

The master functions $\tilde{\phi}_A(\tilde{t})$ and $\tilde{\chi}_A(\tilde{\omega})$ are given by the structure at the critical point. They are independent of the separation parameter σ. The strong control-parameter dependence of the α-process is entirely due to that of its scale τ, referred to as the second critical scale or α-scale. The scaling laws (8) have often been observed in classical research on structure relaxation, where they are referred to as time–temperature superposition principles.

The α-relaxation master functions depend on the probing variable A and therefore no generally valid expression can be given. Generically, the master correlators decay exponentially for very large rescaled or reduced times $\tilde{t}$: $\tilde{\phi}_A(\tilde{t} \to \infty) = \mathrm{O}(\exp(-\Gamma_A\tilde{t}))$. This implies a regular small-frequency susceptibility spectrum $\tilde{\chi}_A''(\tilde{\omega} \to 0) = \mathrm{O}(\tilde{\omega})$. For small rescaled times the von Schweidler expansion, equations (3), holds:

$$\phi_A(\tilde{t} \to 0) = f_A^c - h_A\tilde{t}^b + \tilde{h}_A\tilde{t}^{2b} + \cdots.$$

This is equivalent to a fractal high-frequency α-peak tail $\tilde{\chi}_A''(\tilde{\omega} \to \infty) \propto 1/\tilde{\omega}^b + \mathrm{O}(1/\tilde{\omega}^{2b})$. In the limit of large wave-vectors, $q \to \infty$, the master functions approach Kohlrausch's law, $\phi_K(\tilde{t}) = f_K \exp(-\gamma_K\tilde{t}^{\beta_K})$, where the stretching exponent β_K equals the von Schweidler exponent b: $\tilde{\phi}_q(\tilde{t}) \sim f_q^c \exp(-\gamma_q\tilde{t}^b)$ [71]. Therefore it is a plausible assumption, which is supported by representative numerical solutions of MCT equations, that the Kohlrausch function is a reasonable fit to the major part of the master function $\tilde{\phi}_A(\tilde{t})$. However, the probing-variable-dependent Kohlrausch exponent β_K, as opposed to the von Schweidler exponent b, does not have a precise meaning. It is merely a convenient number quantifying the α-decay stretching. If the density correlators are fitted to Kohlrausch's law, the exponent β_q varies with

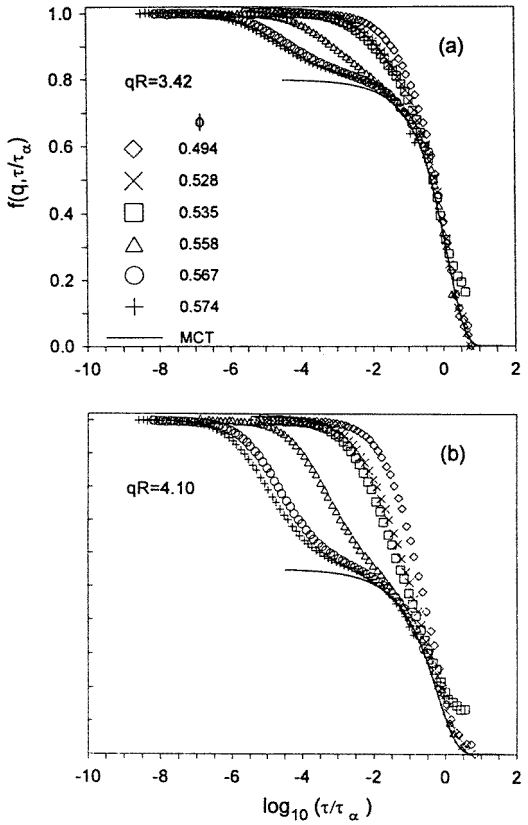

Figure 17. Density correlators $\phi_q(t) = f(q, \tau/\tau_\alpha)$ for various packing fractions φ measured by photon-correlation spectroscopy for a hard-sphere-colloidal suspension as functions of the logarithm of the rescaled times $t/\tau_\alpha = \tilde{t} = \tau/\tau_\alpha$. The rescaling time τ_α is fitted for each φ such that the correlators are superimposed for long times. The full curves show the MCT master functions $\tilde{\phi}_q(\tilde{t})$ of the α-process for the HSS. The peak of the structure factor S_q is located near $qR = 3.5$. Reproduced from reference [72].

wave-vector. In the large-wave-vector limit one gets $\beta_q \to b$. This prediction found support in molecular dynamics simulation results obtained for water [45].

It was shown for a set of wave-vectors that the measured correlators for the hard-sphere colloids obey the scaling law (8*a*). The predicted master functions $\tilde{\phi}_q$, which exhibit a considerable q-dependence, account for the shape of the measured decay curves within a time window larger than two orders of magnitude [27]. Figure 17 [72] illustrates this finding. The decay curves, measured for the colloid of polysterene-micronetwork spheres, mentioned above in connection with figure 10, demonstrate α-scaling for the long-time decay for a three-decade window [66]. Also the correlators for translational and rotational motion obtained for the simulations of a liquid of linear molecules obey the α-scaling law—again with the exception of the ones dealing with angular momentum index $\ell = 1$—and figure 7 exhibits an example. The superposition principle has been confirmed for simulations done for the LJM [28–30] and for water [41, 43–45]. An example relating to the latter results is shown as figure 8.

The left-hand panel of figure 18 reproduces susceptibility spectra measured by depolarized light scattering spectroscopy for OTP [63]. The α-peak has been detected within the accessible

dynamical window for temperatures above 320 K. Optimal fits of the α-peak with Kohlrausch susceptibilities are shown by the full curves. The Kohlrausch exponents β_K found decrease somewhat with increasing T but they are constant within the experimental uncertainties for $T > 360$ K. Uncertainties of the β_K are caused by the ambiguity concerning the decision as to which part of the peak should be used for the fit. If one erroneously includes a part of the β-process in the α-peak, for example, one gets a Kohlrausch exponent which decreases with increasing T. Indeed, the right-hand panel exhibits the validity of the superposition principle and the possibility of describing the upper half of the peak by a Kohlrausch function with a temperature-independent $\beta_K = 0.78$. This exponent differs from the von Schweidler exponent $b \approx 0.6$, determined in reference [63] from the β-relaxation master curve. The α-scaling for OTP density correlators, determined by coherent neutron scattering spectroscopy, is demonstrated in figure 19 [73]. A description of the master functions by Kohlrausch laws is shown by the curves. The exponents $\beta_K = 0.64 \pm 0.03$ for $q = 1.45$ Å^{-1} and $\beta_K = 0.56 \pm 0.03$ for $q = 1.20$ Å^{-1} are different for different q, and both differ from the stretching exponent identified for the light scattering data shown in figure 18. The fact that the long-time decay is more stretched for $q = 1.20$ Å^{-1} than for $q = 1.45$ Å^{-1} is obvious from the data without fitting or rescaling analysis, as was shown in reference [73] by plotting the two measured decay curves for the two cited wave-vectors in one diagram.

The scaling law is derived as an asymptotic-limit result for $\sigma \to 0-$. Thus, the window of rescaled times $\tilde{t} = t/\tau$, where $\phi_A(\tilde{t})$ agrees with $\tilde{\phi}_A(\tilde{t})$, has to expand towards shorter $\tilde{t}$ if T decreases towards the critical temperature T_c or if φ increases towards the critical packing fraction φ_c. Similarly, the window for rescaled frequencies $\tilde{\omega} = \omega\tau$, where equation (8*b*) holds for the data, has to expand to higher $\tilde{\omega}$ for $\sigma \to 0-$. Verification of this manifestation of the asymptotics is an essential step in every test of the MCT results (8). Figures 17, 18, and 19 show examples of this phenomenon. The violations of the scaling shown for short $\tilde{t}$ in figures 17 and 19 and for high $\tilde{\omega}$ in figure 18 are caused by the crossover from the initial von Schweidler part of the α-process to the critical decay. This deviation is described by the β-relaxation results of MCT, as was demonstrated explicitly for the hard-sphere colloid in reference [27], for the micronetwork-sphere colloid in reference [66], for the OTP spectra in reference [63], and for the OTP neutron scattering functions in reference [15].

Let us assume—for the sake of simplicity—that the α-process can be described by a Kohlrausch function $\phi(\tilde{t})/\phi(\tilde{t} = 0) = \exp(-\gamma_K \tilde{t}^{\beta_K})$. Validity of the scaling law means that the stretching exponent β_K is temperature independent. The MCT prediction of asymptotic scaling means that for $T > T_c$ the exponent β_K varies smoothly with T: $\beta_K(T) = \beta_0 + \beta_1(T - T_c) + \cdots$. So up to which values of $T - T_c$ can one expect to find $\beta_K(T) \approx \beta_0 < 1$? All numerical solutions of MCT equations published so far show that the α-peak moves to higher frequencies with increasing $|\epsilon|$ without serious variation of the stretching exponent until the peak merges with the band of microscopic excitations. Indeed, the α-processes of all systems, which could be measured for temperatures above the critical one, evolve in agreement with the scaling law (8), i.e. with a nearly temperature-independent stretching exponent β_K. This holds in particular for the α-peaks of CKN measured by light scattering [50] and by dielectric-loss spectroscopy [18] for temperatures up to $T_c + 60$ K, of glycerol measured by light scattering spectroscopy up to 70 K above the melting temperature T_m [74] and by dielectric-loss spectroscopy up to 30 K above T_m [75], and for PC measured by light scattering spectroscopy [54] up to $T_m + 130$ K and by dielectric-loss spectroscopy [55] up to $T_m + 30$ K. Dielectric-loss spectra for frequencies below 1 GHz often exhibit an α-peak stretching which increases with decreasing temperature, and with a reasonable accuracy this stretching can be parametrized by a Kohlrausch exponent $\beta(T)$ which increases with heating. Extrapolating this trend it has been concluded occasionally that $\beta(T)$ approaches unity for

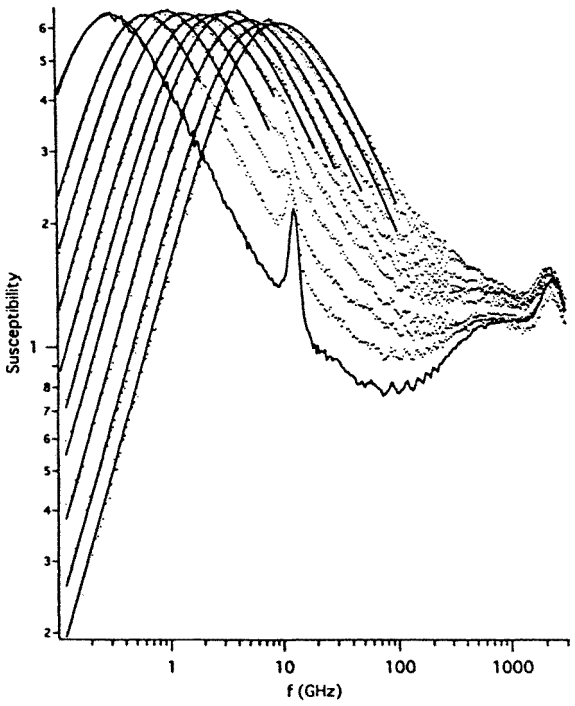

Figure 18. A double-logarithmic representation of the susceptibility spectra $\chi''(\omega)$ of OTP as functions of the frequency $f = \omega/2\pi$ measured by depolarized light scattering spectroscopy. The data in the panel on this page refer to the temperatures $T = 320$, 330, 340, 350, 360, 370, 380, 395, 415, 435 K (from left to right). The full curves are fits with Kohlrausch functions where the stretching exponent β_K decreases from about 0.87 for $T = 320$ K to about 0.75 for $T = 360$ K and it is 0.76 ± 0.02 for larger temperatures. The panel on the facing page shows the spectra as functions of the rescaled frequency $f/f_{\max}$, where $f_{\max}$ is the position of the susceptibility maximum determined by the fits in the panel on this page. The smooth curves with labels $\beta_K = 0.78$ and 1.0 are Kohlrausch spectra with the corresponding exponents β_K. Reproduced from reference [63].

T near the melting temperature T_m. These experimental results are not in contradiction to MCT, since the above-mentioned spectra relate to relaxation below T_c, while the α-scaling law was derived within MCT for $T > T_c$. However, the extrapolations of $\beta(T)$ to unity for $T > T_c$, i.e. extrapolations to temperatures where the α-peak occurs in the GHz band, have been shown to be incorrect in those cases for which the dielectric-loss spectra have been measured [18, 55, 75].

For very high temperatures above some T^*, structural-relaxation anomalies should be absent; relaxation should be a stochastic process characterized by $\beta_K(T \geqslant T^*) \approx 1$. In this sense β_K has to eventually increase to unity upon heating. This approach of $\beta_K \to 1$ is demonstrated for the simulation data of a LJM in reference [28] and for the results of a molecular liquid in reference [39]. In both cases $T^* > 2T_c$. Thus T^* is so large that it is not relevant for structural-relaxation research.

5.2. The second critical timescale

The control-parameter-sensitive timescale τ, which enters von Schweidler's laws, equations (3*a*), (3*b*), and the scaling laws, equations (8*a*), (8*b*), is not identical with the first critical

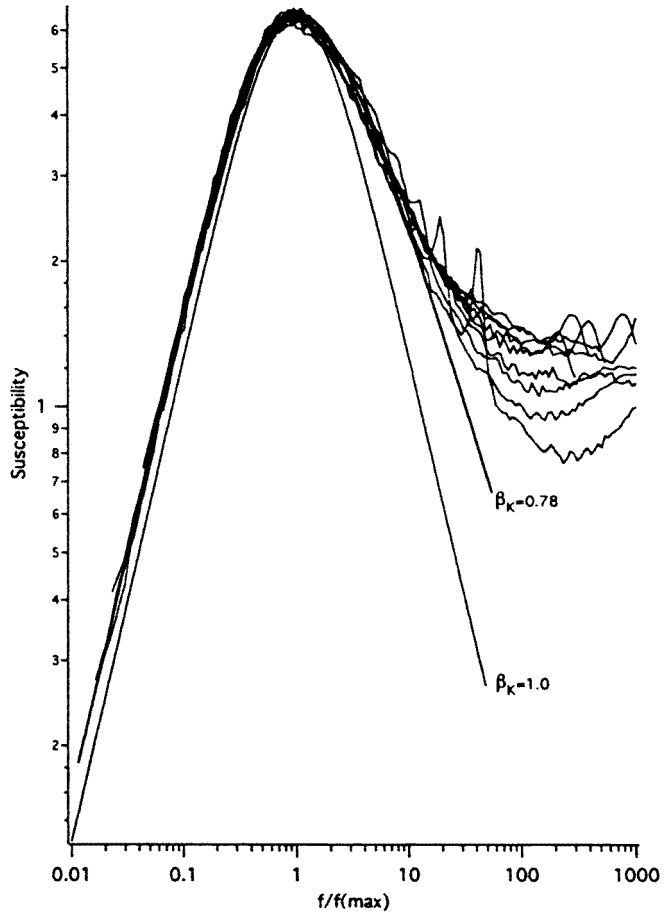

Figure 18. (Continued)

scale t_σ, contained in equation (7). The ideal MCT again yields a power-law divergence but the corresponding exponent γ is larger than the exponent $1/(2a)$ entering t_σ:

$$\tau = B^{-1/b} t_0/|\sigma|^\gamma \qquad \gamma = [1/(2a) + 1/(2b)]. \tag{9}$$

The scale t_0 is the same as in equations ($2a$), (7) and B is a number of order unity given by λ. Formula (9) is an asymptotic result. It becomes invalid if $|\sigma| \propto (T - T_c)/T_c \propto (\varphi_c - \varphi)/\varphi_c$ is too large since in this case the state is too far from the glass transition singularity. But it becomes invalid also if $|\sigma|$ is too small, since hopping effects, which are ignored in the ideal MCT, prevent the system from reaching the singularity. These hopping processes cut off the τ-divergence. The specified complications make it hazardous to apply the formula $1/\tau \propto |T - T_c|^\gamma$ to obtain a fit to data using both T_c and γ as free parameters. The parameters T_c and γ of a fit attempt are strongly correlated and depend on the temperature interval chosen for a fit. The scale is determined best by verifying the scaling equations (3), (8), as demonstrated above in figures 7, 8, 17, 18, and by taking τ from the required shifts parallel to the $\log t$ or $\log \omega$ axis. But signal-versus-noise problems are not so severe for the α-process as for the β-dynamics. For example, from figure 10 one can deduce directly a characteristic timescale τ_α via $\phi(\tau_\alpha) = 0.5$, and from susceptibility spectra in figure 18 one can read off the position

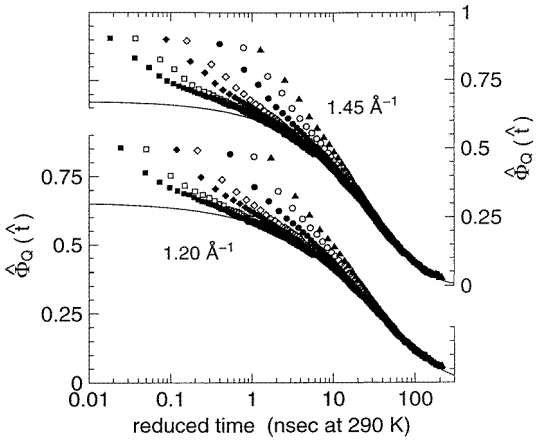

Figure 19. Density correlators ϕ_q for two wave-vectors measured by coherent neutron scattering spectroscopy for OTP as functions of the reduced times $\tilde{t} = t/\tau_s$. The data refer to the temperatures T = 313, 320, 330, 340, 360, 380, 400 K (from left to right). The scaling time is given by $\tau_s = \tau_\eta(T)/\tau_\eta(T = 290\ \mathrm{K})$, where $\tau_\eta = \eta(T)/T$ is the α-scale of the shear viscosity η. The full curves show Kohlrausch functions with stretching exponents 0.64 (upper curve) and 0.56 (lower curve). Reproduced from reference [73].

$\omega_{\max}$ of the α-peak; then one gets $\tau \propto \tau_\alpha$ or $\tau \propto 1/\omega_{\max}$.

The α-peaks shown in the top panel of figure 9 lead to the times $\tau'_\alpha \propto \tau$, represented as filled circles in figure 13; and the line through the data is the power law, equation (9), with the exponent $\gamma = 2.9$; this value corresponds to the result for the exponent parameter $\lambda = 0.81$ of the preceding analysis of the spectral minimum [50]. Formula (9) describes the data for the two-orders-of-magnitude shift of the α-peak which was observed in this experiment. The same conclusion was arrived at for the analysis of the OTP results shown in figure 18 [63] as well as for the scales of the α-processes measured by light scattering for Salol [47] and PC [54]. The findings for Salol were corroborated by the analysis of time-resolved optical Kerr-effect results: the α-scaling law was confirmed for T between 293 and 363 K and the scale followed the power law, equation (9), with T_c and γ consistent with the other cited findings [48]. As discussed above for the β-relaxation scales, it is more practical to test the power-law behaviour using a rectification diagram. The interpolation using a straight line of the $\tau^{-1/\gamma}$-versus-T data set yields a further estimate of T_c. For the cited examples [47, 50, 54, 63] the results are consistent with the previously discussed findings for the crossover temperature obtained from the β-relaxation scaling analysis. Similarly, the $\nu_{\max}^{1/\gamma}$-versus-T diagrams, deduced for the dielectric-loss data for PC [55], corroborated the values of γ and T_c obtained by the β-relaxation analysis of results for other probing variables [54,56]. The lowest panel of figure 12 demonstrates such an analysis of the CKN data for the α-peak frequency $\nu_{\max}$ deduced from dielectric-loss spectroscopy [37].

The dashed curve in figure 14 shows the power law $\tau \propto (\varphi_c - \varphi)^{-\gamma}$ with the value $\gamma = 2.6$ calculated for the HSS. It describes the variation of τ over more than three orders of magnitude for $\sigma > -0.1$ as observed for the α-process of the density fluctuations for the hard-sphere colloid [33]. For this system the critical point is determined so well that it is adequate to present the data as a log τ-versus-log $|\epsilon|$ diagram; $|\epsilon| \propto |\sigma| \propto (\varphi_c - \varphi)/\varphi_c$. Such a diagram is shown in figure 20, where recently measured relaxation times for a tagged-particle-density correlator and for the diffusion constant D are also included [76]. The transport coefficient D

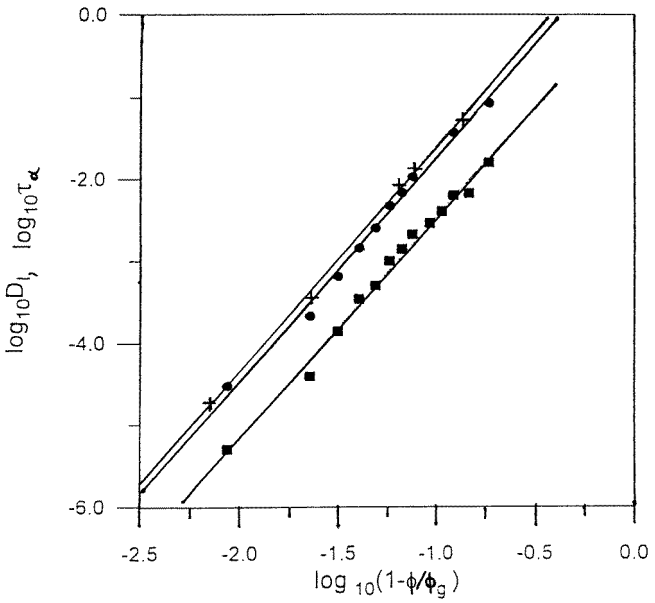

Figure 20. Double-logarithmic plots of the diffusivity (squares), α-relaxation rates $1/\tau$ of a tagged-particle-density correlator (circles), and α-relaxation rates $1/\tau_\alpha$ for a density correlator (crosses) versus $(\varphi_c - \varphi)/\varphi_c$. The data are determined from photon-correlation spectroscopy results for a hard-sphere colloid. The straight lines interpolate the data sets with a slope $\gamma = 2.7$. Reproduced from reference [76].

is proportional to the time τ for the α-process of the mean squared displacement. The data in figure 20 follow straight lines, thus confirming power-law variation. The slope is the exponent γ for which the predicted HSS value 2.6 is confirmed within a 5% uncertainty in all three cases.

For the relaxation curves of the polysterene-micronetwork-sphere colloids, shown in figure 10, an increase of the timescale τ by about five orders of magnitude is observed. It follows the power law with exponent $\gamma = 3.6$, which corresponds to the exponent parameter $\lambda = 0.88$ deduced from the preceding β-relaxation scaling verification [51].

The analysis of the simulation results for the density fluctuations of water [43, 44], mentioned above in connection with figure 8, identified the value $b = 0.50$ for the von Schweidler exponent. From equation (9) one calculates an exponent $\gamma = 2.7$ for the power-law exponent for the asymptotic variation of the diffusivity: $D \propto (T - T_c)^\gamma$. This formula is consistent with the simulation data and accounts for a variation of the diffusivity over three orders of magnitude [44]. The simulation provided also the α-relaxation timescales τ_ℓ for the reorientational correlators for angular momentum index $\ell = 1, \ldots, 5$. The rectification diagram confirmed the cited power-law behaviour with a value of T_c consistent with all of the other estimates for the crossover temperature [46]. The data exhibit a trend for $1/\tau$ to be smaller than the power-law extrapolation if $T - T_c > 60$ K. These deviations from the asymptotic law are largest for τ_1. Equation (9) was also tested and confirmed for the coherent and incoherent density correlators obtained by molecular simulations for a LJM [28–30] and for the cited model for a molecular liquid [38–40]. However, for both systems the diffusivity D did not exhibit the predicted behaviour. It was already mentioned that the reorientational correlators for the linear molecules for angular momentum index $\ell = 1$ did not exhibit the

α-scaling law and therefore it is not surprising that they did not follow the predicted power law of the α-relaxation scale either.

5.3. The α-scale coupling

Consider some variables, say A and B, coupling to density fluctuations, and let us denote their α-relaxation times by τ_A and τ_B respectively. If, e.g., A is the shear stress and B a fluctuating force acting on a tagged particle, $\tau_A = \tau_\eta$ and $\tau_B = \tau_D$ are timescales for the variation of the viscosity η and diffusivity D respectively. The conventions for the definition of the scales might be different from the one used above. But equations (8) imply the prediction of the α-scale coupling: $\tau_A = C_A\tau$, $\tau_B = C_B\tau$ where τ is the second critical scale. The coefficients C_A, C_B are smooth functions of control parameters and thus they can be treated as constants in a leading-order asymptotic expansion. Scale coupling is demonstrated in figure 20 [76]. It shows a comparison of three scales, namely the ones for coherent density fluctuations, for tagged-particle-density fluctuations, and for diffusion in hard-sphere colloids: the measured scales vary by about a factor of 1000, but the logarithm of their ratios, i.e. the distances between the lines in the figure, are independent of the packing fraction φ.

The α-scaling plot for the OTP neutron scattering data in figure 19 was obtained with the α-scale for the viscosity [73]. Thus the figure demonstrates the coupling of the scale for the measured density fluctuations with microscopic wavelengths to the timescale τ_η for shear fluctuations with macroscopic wavelengths. The viscosity of OTP follows reasonably well the power law (9) with $\gamma = 2.5$ [4], and this agrees within the experimental uncertainties with the exponent $\gamma = 2.8$ derived from the scaling-law analysis of the depolarized light scattering spectra [63]. The coupling of the α-scale measured by depolarized light scattering for Salol to the viscosity scale was demonstrated in reference [47]. The proof that the scale of the two variables follows the law $(T - T_c)^\gamma$ with compatible T_c and γ implies the proof of the coupling. Thus the results discussed above for PC and CKN exemplify scale coupling and so do the results cited in section 5.2 for the various molecular simulations.

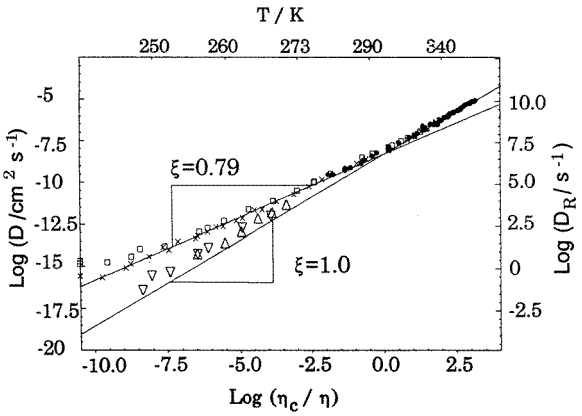

Figure 21. The rotational diffusivity D_R (triangles) and translational diffusivity D versus the reciprocal viscosity η in a double-logarithmic representation. The dots refer to self-diffusion, the squares and crosses to the diffusivity of tracer molecules in OTP. The slope $\xi = 1$ demonstrates scale coupling and $\xi \neq 1$ decoupling. Reproduced from reference [77].

The coupling of scales is not trivial, contrary to what is sometimes suggested by appeal to the Stokes–Einstein- or Stokes–Debye-relation formulae. For $T < T_c$ relaxation is due

to thermally activated processes. There is no reason for the activation energy for diffusion, relating to hops of a single particle over saddle points in the potential landscape, to be the same as the one for the viscosity, which relates to the coherent motion of many particles. Coupling of the scales τ_D and τ_η would mean that the log D-versus-log$(1/\eta)$ curve has a slope $\xi = 1$. But figure 21 [77] shows that this slope is about 0.79 for low temperatures in OTP. Decreasing T from 290 K to about 250 K implies a variation of τ_D/τ_η by about a factor of 100. The critical temperature T_c for this system, established by the neutron and light scattering experiments cited above, is 290 ± 10 K. Thus figure 21 demonstrates decoupling of scales for $T < T_c$. The MCT prediction of scale coupling refers to the regime $T > T_c$, and indeed for the nearly three-orders-of-magnitude scale variation for $T > T_c$, documented in figure 21, the scale coupling $\xi = 1$ is confirmed. An addition to the preceding discussion might be in order. If the tagged particle is chemically identical to the liquid particles, D is called the self-diffusion constant. If it is different, e.g. some dye molecule, D is often referred to as the tracer diffusivity. Thus the filled circles in figure 21 demonstrate scale coupling for the self-diffusion for $T > T_c$, and the open squares demonstrate scale decoupling for a tracer diffusivity for $T < T_c$. The cited scale coupling is derived in MCT under the assumption that the tagged-particle–host-particle coupling is sufficiently strong. If this coupling decreases below a critical value, the possibility of a glass for $T \leqslant T_c$ containing non-localized tracer particles arises. This state is a model, for example, for a conducting glass. For such small tracer–host couplings, the tracer diffusivity D does not decrease to zero proportionally to $1/\eta$ if T decreases towards T_c; hence for such a case, scale coupling is not predicted.

The most sensitive test of scale coupling is a plot of the ratio of the two scales $\tau_A/\tau_B = C$ as function of the control parameter. A plot of τ_η/τ_D versus T for OTP data [78] corroborates the findings demonstrated in figure 21. Exactly the same behaviour is exhibited by the (τ_η/τ_D)- and $(\tau_\eta/\tau_\epsilon)$-versus-$T$ plots of Salol, where τ_ϵ is the α-relaxation scale for the dielectric-loss peak: the scales are coupled for $T > T_c$ and they decouple for temperature below T_c [79]. The scale coupling is a prediction valid for parameters so close to the transition singularity that the non-linear mode-coupling effects dominate the dynamics. The asymptotic formulae do not imply predictions for T far above T_c or φ far below φ_c. Indeed, for the hard-sphere colloids the ratio $C = \tau_D/\tau_\eta$, which should be constant if the Stokes–Einstein formula is to be correct or if scale coupling is to be valid, decreases from 6 to 4 if φ increases from zero to 0.5 [80]. It would be interesting to know whether this ratio C becomes independent of φ in the interval $0.5 < \varphi < \varphi_c$, where the other cited experiments for the hard-sphere colloids show the dominance of mode-coupling effects.

The exponent $b \approx 0.49$ was estimated for the simulation data for a LJM by verification of von Schweidler's law; also the validity of the superposition principle was confirmed. From this von Schweidler exponent one obtains the MCT prediction $\gamma \approx 2.6$. The α-relaxation scales for density fluctuations are consistent with the predicted power law with the cited value for γ, as shown in figure 22. However, the scales for the diffusivities of the particles do not lead to a straight line running parallel to the first one in this diagram [28]. A similar violation of MCT α-scale asymptotics was reported for the simulation data for a molecular liquid [39].

Brillouin-scattering spectroscopy is a technique which explores the implications of structural relaxation for hydrodynamic excitations. A Brillouin-scattering spectrum is determined by the longitudinal elastic modulus $M(\omega)$. The spectrum is dominated by the scattering resonance whose position ω_B and width are given by $M(\omega_B)$. It is practically impossible to determine from the data the frequency dependence of $M(\omega)$ for a sufficiently large dynamical window to allow one to examine the evolution of structural relaxation. To interpret the spectra, one has to impose some model for $M(\omega)$ and then use fits to the data for the determination of the model parameters. Traditionally, an α-process-only model has been studied: a white-

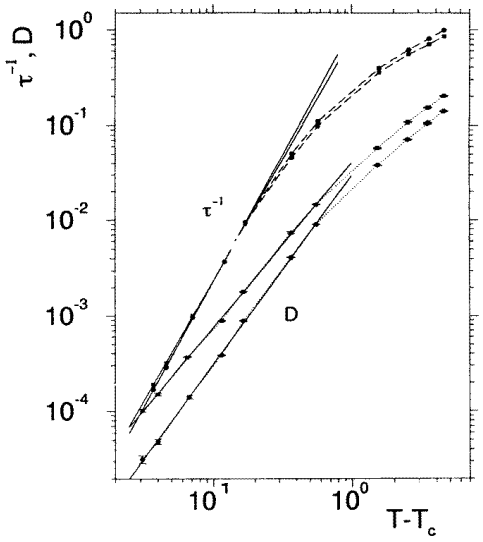

Figure 22. Double-logarithmic representations of the inverse relaxation times $1/\tau$ (dashed curves) and diffusivity D (dotted curves) for A particles (circles) and B particles (squares) obtained by molecular dynamics simulations for a LJM as functions of $T - T_c$. The straight-line interpolations represent power laws with exponents given by the slopes. Reproduced from reference [28].

noise background plus an α-process fit formula, obtained, e.g., from a Kohlrausch function $f_K \exp(-t/\tau_K)^{\beta_K}$. Repeatedly it has been reported as a result of such studies that β_K and τ_K/τ_η increase with increasing temperature, i.e. results which suggest a violation of the time–temperature superposition principle and of the α-scale coupling respectively. However, the specified model ignores the possible existence of the MCT β-process. If for $T \sim T_c$ the modulus were to exhibit the spectral enhancement between the α-peak and the microscopic-excitation band which was detected for all of the other measured functions cited in section 4, the α-peak tail alone would underestimate $M''(\omega_B)$ and incorrectly describe the temperature dependence of $M(\omega_B)$. The fit would compensate for this defect by readjusting β_K and τ_K/τ_η and this by different amounts for different temperatures T. This problem was recognized and discussed in detail for CKN data in reference [14]. It was concluded that the fit parameters τ_K and β_K, which are based on α-process-only models, are not generally meaningful. It was shown, in addition, that the apparent temperature dependence of τ_K/τ_η and β_K was eliminated for CKN after some estimate of the critical spectrum for the modulus was included in the model for $M(\omega)$. A similar result could be obtained by an *ad hoc* addition of some spectral bump to the α-peak of $M''(\omega)$, located in the GHz band and described, e.g., by an essentially temperature-independent Debye peak. At present it is not possible to discriminate between the indicated models for the data analysis. Consequently, the previously reported fit results β_K, f_K and τ_K for Brillouin-scattering spectra cannot be used for an assessment of MCT.

6. The evolution of structural relaxation

In a leading-order treatment of the MCT dynamics, using the separation parameter σ as a small quantity, the long-time limit of the first-scaling-law description of the correlators is identical with the short-time limit of the second-scaling-law description. Therefore the two results can be spliced together to provide a complete description of the structural relaxation near the

glass transition singularity. The deviation from the α-relaxation scaling on the high-frequency wing of the susceptibility peak, which is demonstrated by the right-hand panel of figure 18, was explained by the β-relaxation scaling-law results in reference [63]. Similarly, the large violations of the superposition principle for short rescaled times, which are demonstrated in figure 17, were explained quantitatively in reference [27] using the β-relaxation formulae. The violations of the β-scaling for small frequencies, which are obvious in the bottom panel of figure 9, are explained by the theory for the α-process [50]. This subtle interplay of α- and β-dynamics is connected with the appearance of two critical timescales t_σ and τ. Both diverge within the ideal MCT upon cooling or compressing the system, but their ratio diverges as well: $\tau/t_\sigma \to \infty$ for $\sigma \to 0-$. This phenomenon is demonstrated by the data in the top panel of figure 9. The frequencies for the spectral minima $\omega_{\min}$ and maxima $\omega_{\max}$ decrease strongly with cooling, but the ratio $\omega_{\max}/\omega_{\min}$ also decreases by about a factor of 5 if T decreases from 195 °C to 140 °C. The increase of τ/t_σ can be inferred from the raw data in the time domain only if the system is so close to the transition singularity that the plateau f_q^c is obvious. Then the increase of τ, given by $\phi_q(\tau)/f_q^c = 0.5$, relative to $t_- \propto t_\sigma$, given by $\phi_q(t_-) = f_q^c$, can be read off directly. The ratio τ/t_σ for the data in figure 10 varies by more than two orders of magnitude [51]. The predicted two-step-relaxation scenario—the first step governed by the dynamics on the scale t_σ and the second step by the dynamics on the scale τ—is tested and confirmed by all of the studies quoted in the preceding two sections, where for a given material a simultaneous consistent analysis of the α- and β-relaxation with MCT formulae proved possible. This conclusion can be corroborated by splicing together the results of the α-relaxation fit with the β-relaxation fit to a combined α–β fit of the whole structural-relaxation pattern.

Figure 23 [27] shows as full curves for $\varphi < \varphi_c$ the results of a combination of α- and β-relaxation results for the HSS, where the predicted values for the exponent parameter λ and for the normalized theoretical master functions $\tilde{\phi}_q(\tilde{t})/f_q^c$ have been used as input. Analogous figures for three additional wave-vectors are published in references [27, 33]. The amplitudes f_q^c, h_q entering the analysis had been found to agree with the predicted values as shown in figure 3. The separation parameter σ, entering the various scales, was found to vary as $\sigma = C(\varphi - \varphi_c)/\varphi_c$ with $C \approx 1.2$ being consistent with the predicted value for both $\varphi < \varphi_c$ and $\varphi > \varphi_c$ [72]. The ratio τ/t_σ of the two critical timescales varies by more than a factor of 20, as is demonstrated in figure 14. Besides the scale t_0 for the transient motion, which is a number determined by the viscosity of the solvent, there entered as a fit parameter only the critical packing fraction φ_c. The value φ_c had to be adjusted here, as in any other test of a singularity theory, to match to the experimental transition point (compare section 2.2). The quoted results demonstrate that the description achieved for the evolution of glassy dynamics extends over four to five decades in time, holds for a significant range of q-values, and holds for α-relaxation times that vary over four orders of magnitude [81]. Therefore the cited results imply that MCT provides a first-principles understanding of the HSS glass transition as far as it manifests itself in the density-fluctuation dynamics.

Ever since Maxwell's invention of the theory of visco-elasticity, the behaviour of shear has been of interest in the discussions of glassy dynamics. Also, for a hard-sphere-colloidal suspension the dynamical shear modulus $G(\omega)$ was measured for large packing fractions using a Cuette viscosimeter [82]. The data analysis is complicated by the fact that the microscopic-excitation spectrum exhibits an $\omega^{1/2}$-anomaly. The data extend over a four-decade frequency window, and they can be explained using the MCT scaling-law formulae for the HSS β-process. It was emphasized that neither the evolution of the measured plateau of the reactive part $G'(\omega)$ nor the minimum of the dissipative contribution $G''(\omega)$ can be understood without the use of MCT results [82].

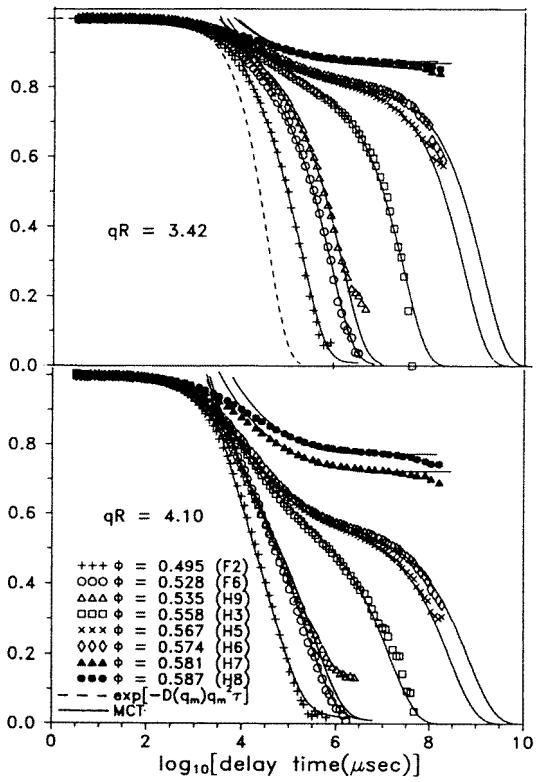

Figure 23. Density correlators $\phi_q(t)$ for two wave-vectors q as functions of $\log_{10}(t)$ measured for various packing fractions φ by photon-correlation spectroscopy for a colloidal suspension of hard spheres with radius R. The main maximum of the structure factor for the packing fraction at the freezing point $\varphi_f = 0.494$ is located at $qR = 3.46$. The dashed curve in the upper panel is the exponential $\exp[-q^2 D(q)t]$ with $D(q)$ denoting the short-time diffusivity. The full curves for $\varphi < \varphi_c$ are fits using the combination of the leading-order asymptotic results for the α- and β-processes predicted by MCT for the HSS. The full curves for $\varphi > \varphi_c$ are fits by the MCT results for the β-process. Reproduced from reference [27].

A combined α–β analysis for correlation functions of a colloid of polysterene-micronetwork spheres has been presented in reference [61]. It accounted well for the evolution of the structural relaxation for this system, which extended over an enormous dynamical window of seven orders of magnitude. The system under discussion is a candidate for treatment via a first-principles MCT calculation. However, it was shown that the structure factor S_q is rather different from that of a simple Lennard-Jones system. The variation of S_q due to changes of the packing fraction φ does not follow the pattern familiar from the discussion of the cage effect: with increasing φ the peak height can decrease [83]. It is not known which interaction causes such behaviour. Therefore one cannot meaningfully extrapolate the measured S_q over the whole q-range, a prerequisite for microscopical calculations of, e.g., the exponent parameter λ.

For complicated systems like CKN and OTP, first-principles MCT results are not yet available. Therefore a data analysis has to use the theoretically well defined parameters $\lambda, C, T_c, f_A^c, h_A, t_0$ as fit quantities, as was anticipated already in connection with the various MCT interpretations reported above for these systems. Figure 24 represents a summary of an

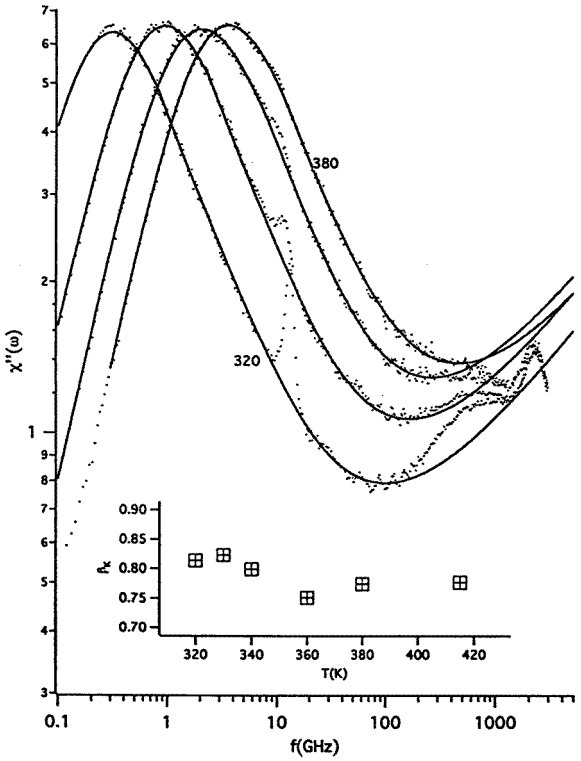

Figure 24. Double-logarithmic representations of the susceptibility spectra $\chi''(\omega)$ as functions of the frequency $f = \omega/2\pi$ obtained by depolarized light scattering spectroscopy for OTP for temperatures $T = 320$, 340, 360, and 380 K. The full curves are combinations of fits with the MCT formulae for the β-relaxation and a Kohlrausch-law fit for the α-peaks with stretching exponents β_K shown in the inset. Reproduced from reference [63].

exhaustive analysis of the depolarized light scattering data for OTP [63]. For splicing together the two scaling-law formulae, the α-relaxation master function was modelled by a Kohlrausch law. It is characterized by the stretching exponent β_K. The inset shows that β_K is constant within the experimental uncertainties. The structural-relaxation spectra shown extend over a window of three-orders-of-magnitude variation of frequency f below 0.1 THz. For larger frequencies the dynamics is influenced by oscillatory motion, which is not treated by the various asymptotic formulae. Frequencies below 0.1 GHz are not accessible with the tandem Fabry–Pérot spectrometer and therefore for temperatures below 320 K the α-peak maximum is not visible any longer. The data for these lower temperatures have been analysed by using the β-relaxation theory alone, albeit by the one of the extended MCT [63]. The numbers λ and T_c identified are consistent within the experimental uncertainties with the values used to describe the results of the neutron scattering research, as can be inferred from reference [15] and the papers quoted there. The exponent γ for the α-relaxation timescale is known to describe adequately the viscosity variation of OTP [4] and, because of the scale coupling demonstrated in figure 21, it also agrees with the exponent used in describing the temperature variation of the translational and rotational diffusion for $T > T_c$.

There is also a test of MCT results based on depolarized light scattering spectra of OTP that was carried out for a 90° scattering geometry [84]. It was shown that the measured

spectral minima can be interpreted with the MCT β-relaxation formulae using values for T_c and λ consistent with the ones known from the preceding neutron scattering studies. But two objections against the applicability of the theory have been formulated. First, it is reported that the Kohlrausch exponent β_K for the α-peak increases with temperature for $T > T_c$ such that it is nearly unity for $T \geqslant 320\ \mathrm{K} = T_c + 30\ \mathrm{K}$. It was argued that the MCT prediction for $T > T_c$ of an essentially temperature-independent Kohlrausch exponent β_K is 'in contradiction to the experimental data' [85]. However, the authors define their α-peak differently to how it is done in MCT. Instead of using the measured peak directly, they first subtract a Debye peak from their spectra. Moreover, the applied fit procedure is unstable and it can be used, with an even better confidence level, also to derive a fit with a temperature-independent β_K [86]. The second objection concerns the statement that the minima positions $\omega_{\min}$, which are obtained from an analysis of the β-scaling, differ from the minima obtained from a data interpolation by an even polynomial in $\xi = \log(\omega/\omega_{\min})$: $\chi''(\omega) - \chi_{\min} = A_2\xi^2 + A_4\xi^4 + A_6\xi^6$. But the data in reference [84] do not suggest the symmetry $y(\xi) = y(-\xi)$, and the MCT result does not exhibit this symmetry either, because $b > a$. It does not seem a reasonable objection against a theory if fits, which interpolate data by a formula which contradicts that theory, lead to some inconsistencies.

7. Various further tests

7.1. Structure and structure relaxation

MCT was derived for strongly interacting amorphous matter. The input information needed for the MCT equations of motion are equilibrium structure factors and these structure factors are assumed to depend smoothly on the wave-vectors and on the control parameters. The cited leading-order asymptotic formulae would not necessarily be correct if there were long-range-order singularities for the wave-vector-dependent compressibility, as one would expect near second-order phase transitions. If there were to be a singularity in some other susceptibility, it would not be of concern for MCT as long as this singularity does not introduce divergences in the mode-coupling integrals. Structure functions which enter MCT are taken from other theories or from experiment. The cited results for the HSS, for example, are based on the Verlet–Weiss theory for S_q. The MCT calculations for the LJM in reference [31] are based on structure factors obtained from molecular dynamics simulations for this system. Studies of the structure factor of OTP showed that S_q varies smoothly if the temperature varies between $T_c - 30\ \mathrm{K}$ and $T_c + 30\ \mathrm{K}$ [15, 87]. Nor does the structure factor of CKN exhibit any anomaly for T near T_c [88]. MCT does not address the question of why systems like OTP or CKN can be kept in a supercooled state while other systems cannot. For both systems the basic assumptions of MCT seem justified.

MCT has shown that the existence of the α-process and its detailed properties for $T > T_c$ can be understood without considering the problem of supercooling. For the explanation of the glassy dynamics of OTP in the GHz window, for example, it is irrelevant that the true equilibrium state for temperatures below the melting temperature $T_m = 329\ \mathrm{K}$ is a crystal. The experiments, which are documented in figures 18, 19, 24, show that the α-process is described by the same master function and that the relaxation scale τ follows the same power law for temperatures increasing from below T_m to 50 K above T_m. Similarly, the α-process of PC was shown by dielectric-loss spectroscopy to follow the MCT prediction for temperatures up to $T_m + 30\ \mathrm{K}$ [55] and by light scattering up to $T_m + 130\ \mathrm{K}$ [54].

In order to keep a dense hard-sphere colloid in an amorphous state it is necessary to allow for a certain percentage P of polydispersity; otherwise the system forms a cubic crystal

for $\varphi > \varphi_f = 0.494$. The Percus–Yevick theory yields a structure factor S_q which varies smoothly with P, and therefore the MCT results, which are based on this S_q, are also robust with respect to changes of the polydispersity. In particular one can use the theoretical results for the monodisperse system to describe the polydisperse sample within the experimental uncertainties, provided that P is not too large. These conclusions are supported by the observation that structural-relaxation properties, as opposed to nucleation phenomena, are insensitive with respect to changes of P [89].

A result of particular importance for the physical interpretation of MCT is the following. The correlators outside the transient can be written as $\phi_q(t) = F_q(t/t_0)$, where the functions F_q are determined completely by the equilibrium structure. The transient dynamics, in particular all details of the underlying microscopical equations of motion, enter via a single timescale t_0 only, which depends smoothly on control parameters. Molecular dynamics simulations are the proper technique to test this general prediction. A possibility is the comparison of data, say for a binary mixture, where for fixed interaction potential the mass ratio of the particles is varied [90]. The details of the normal-liquid dynamics depend on the mass ratio but structural relaxation should not, except for a change of t_0. This is due to the fact that the structure factors of classical liquids are independent of the particle masses; they are determined solely by Meyer factors, i.e. by the ratios of potential and thermal energies. Another possibility for a test is making a comparison of a system obeying Newtonian dynamics with one obeying some stochastic dynamics as was done in reference [91]. Structural relaxation was observed for windows of two to three decades. In contrast to the MCT prediction it was concluded that the Kohlrausch exponents for the α-process description differ significantly for the two models and that the structural-relaxation dynamics depends qualitatively on the nature of the underlying equations of motion considered. However, it is not evident that the cited conclusions are justified by the simulation results published in reference [91]. The α-peaks of the susceptibility spectra for density fluctuations studied for a wave-vector near the position of the structure factor peak agree for a two-decade dynamical window; in particular the two α-peak spectra have the same upper 45%. From this fact one can only conclude that a description by Kohlrausch laws leads to identical stretching exponents β_K within the uncertainty of the data. Similarly, the correlator decays of the two models are 70% identical and this for long times. For the Newtonian dynamics the initial part and the crossover to the structural relaxation shows the same qualitative behaviour as is exhibited by numerical solutions of MCT models. This leads to a bump of the susceptibility spectrum which would cover a possible anomalous spectral minimum, quite similar to the oscillation bump near 400 GHz which masks the critical OTP spectrum for 320 K in figure 24. The solutions of the Brownian-dynamics model, on the other hand, exhibit a stretched decay from 90% to 70%, which yields for the spectrum the crossover from the α-peak to a minimum. The minimum spectral intensity is strongly enhanced above any estimate for a regular white-noise-background spectrum. This finding is the signature of the underlying critical decay. Therefore I conclude that the results of reference [91] support the cited MCT prediction. A discussion of structure relaxation has appeared recently for the LJM, comparing a Newtonian and a stochastic motion model for the equations of motion. The α-scaling plot followed the pattern predicted by MCT; the master functions for the two models are identical and so are the scaling times for sufficiently small $T - T_c$ [36]. Figure 4 shows the comparison of the critical glass form factors obtained for the two models (filled versus open symbols). Thus the formula $\phi_q(t) = F_q(t/t_0)$ has been confirmed completely as far as the α-process is concerned. Furthermore, it was shown for the stochastic dynamics model that for the lowest accessible temperature the correlator approaches and leaves the plateau f_q^c as predicted by the β-relaxation master function $g_-(\hat{t})$ for this system, while for the Newtonian-dynamics model the correlators for $\hat{t} = t/t_\sigma < 1$ are dominated by oscillations.

A facet of the problems discussed in the preceding paragraph is the following. Let us consider models which all have the same interaction. Suppose in addition that there is a minimal separation parameter $\sigma_{\min}$ so that data need to be considered only for $\sigma < -\sigma_{\min}$. In a simulation study, $\sigma_{\min}$ might be determined by the lowest temperature above T_c for which equilibration of the system can be achieved. Then one can choose the microscopical equations of motion such that the transient dynamics masks the critical decay. It is a typical result of MCT solutions that for a certain $\sigma_{\min}$ no critical decay is detectable in the $\phi_q(t)$-versus-log t curves, even though the α-process exhibits the α-scaling law, the von Schweidler decay, and the power-law variation of the α-relaxation scale τ with the proper exponent γ. Thus, the impossibility of identifying the $1/t^a$ law in the published simulation results for a LJM [28–30] or for water [43–45] is not an objection against the applicability of MCT. However, the result described is not universal, and for the experiments discussed in sections 3 and 4 the $1/t^a$ law manifests itself for a $\sigma_{\min}$ which is comparable with the ones studied in the cited simulations. Obviously, it is desirable to invent models for simulation studies which exhibit a critical decay as strongly as is found in several laboratory studies. The simulation results for a system of linear molecules [39] differ from the ones for the LJM or water in the sense that a stretched decay towards the plateau f_q^c is visible. This is demonstrated in figure 7 for the rescaled time t/τ varying between 10^{-4} and 10^{-2}. Indeed, it was shown for translational and rotational correlators for the lowest temperature studied that the decay towards the plateau f_q^c and beneath it can be described by equations (4*a*), (5*a*), where the β-correlator $g_-(\hat{t})$ was evaluated for the exponent parameter $\lambda = 0.76$. Therefore for this model a test of the MCT predictions for the dynamics within the first-scaling-law regime might be possible.

7.2. Empirical fit formulae

There is a long tradition of fitting structural-relaxation data with empirical formulae. Such work implies a challenge for MCT in the sense that the range of validity for the fits and the variation of the fit parameters with, e.g., temperature changes should be explained. Three examples will be considered. First, let us discuss fits of $\phi(\tilde{t})$-versus-log $\tilde{t}$ curves with Kohlrausch functions. If the control parameters are sufficiently far from the critical ones, the curves outside the transient regime exhibit a single inflection point only. This is the case for the data sets in figure 17 for $\varphi \leqslant 0.535$ and for the ones in figure 19 for $T \geqslant 340$ K. In such cases one cannot decide without additional information which part of the curve should be considered as the α-process. A free fit using a Kohlrausch law is likely to include a larger dynamical window than a fit carried out with the constraints provided by MCT. In particular, a free fit for the cited data sets will not lead to the master functions shown as curves in figures 17 and 19. For example, it was shown that such a free fit can account for a set of correlators of hard-sphere colloids as well as a combined α–β-relaxation fit with MCT formulae [92]. Similarly, an unbiased fit with Kohlrausch functions is of comparable quality for the description of solvation dynamics observations to the results of a MCT analysis [56]. These two examples show in particular that a successful fit with stretched exponentials $f_K \exp -(t/\tau_K)^{\beta_K}$ is not necessarily a contradiction to MCT. MCT explains the success of the fit and the observed increase of β_K with decreasing φ or increasing T respectively by the fact that parts of the crossover from the α-decay for $\phi_q(t) < f_q^c$ to the critical decay for $\phi_q(t) > f_q^c$ are included in the analysis. In addition, MCT explains the paradox that a free fit of the corresponding α-peak for the susceptibility spectrum leads to a decrease of the stretching exponent β_K with increasing T. The inclusion of the β-relaxation widens the α-peak, and this implies a decrease of β_K for the unbiased fit. But MCT predicts also that for parameters closer to the critical point the $\phi(t)$-versus-log t curve should exhibit a second inflection point outside the transient regime, as shown for the

data in figure 17 for $\varphi = 0.567$ and 0.574 and for the ones in figure 19 for $T \leqslant 330$ K. These curves cannot be described by a Kohlrausch function and they demonstrate the inferiority of the empirical fit in relation to the one based on theory.

The empirical fit discussed in the preceding paragraph describes the susceptibility minimum as a crossover from the high-frequency α-peak tail, $\chi''(\omega) \propto 1/\omega^{\beta_K}$, to some regular-background spectrum. MCT predicts that for parameters sufficiently close to the glass transition singularity such a description should underestimate the minimum intensity seriously because there is an enhanced background due to the critical spectrum. Indeed, the failure of the empirical approach in such cases, caused by ignoring the critical spectrum, was demonstrated for CKN light scattering spectra for 120 and 150 °C in reference [93] and for the dielectric-loss spectra of glycerol in reference [75].

A second example of an *ad hoc* data-fitting procedure also concerns the minima of the susceptibility spectra between the α-peak and the microscopic-excitation spectrum. Suppose that the high-frequency α-peak tail can be described by von Schweidler's law: $\chi_1''(\omega) = c_1/\omega^b$, $1 \geqslant b > 0$. Let us assume also that the $\log \chi''$-versus-$\log \omega$ graph in the frequency region relating to the low-frequency wing of the microscopic peak can be approximated by a straight line of some slope $a_{\text{eff}} > 0$, i.e. by an effective-power-law spectrum $\chi_2''(\omega) = c_2\omega^{a_{\text{eff}}}$. The crossover from one spectrum to the other produces a minimum at some frequency $\omega_{\min}$ with a certain intensity $\chi_{\min}$. A reasonable approximation for this minimum is given by the interpolation formula

$$\chi_{\text{int}}''(\omega) = \chi_1''(\omega) + \chi_2''(\omega) = \chi_{\min}[b(\omega/\omega_{\min})^{a_{\text{eff}}} + a_{\text{eff}}(\omega_{\min}/\omega)^b]/(a_{\text{eff}} + b).$$

It obeys the β-relaxation scaling law, equation (5*b*), if one assumes that the exponents b and a_{eff} are temperature independent. MCT shows the approximate validity of all of the assumptions made above and thus of the fit formula $\chi_{\text{int}}''(\omega)$. In addition MCT implies the following result: in the asymptotic limit, where the minimum is so far separated from the microscopic-excitation band that there are no spectral tails due to the transient present any longer, the background spectrum is the critical one. The latter is specified by an exponent $a_{\text{eff}} = a \leqslant a_{\max} \approx 0.395$, which can be determined from b. Depolarized Raman-scattering spectra for a window between 40 and about 400 GHz have been analysed for several systems with the cited interpolation formula [94]. For OTP a fit value $a_{\text{eff}} > a_{\max}$ was found. It was claimed that this finding proves MCT to be not correct quantitatively [94]. However, it is known that OTP exhibits a bump in the spectral density $\phi''(\omega)$ due to oscillatory motion, often referred to as a boson peak, which influences the spectra down to 200 GHz as demonstrated in figure 24. This spectrum can increase a_{eff} above a. The asymptotic MCT results for the first- and second-scaling-law regimes relate to structural relaxation only. Those parts of the spectra, like the boson peak contribution, which are modified by oscillation dynamics, must not be included in the windows for the fits with asymptotic results. Indeed, the successful MCT analysis of the OTP spectra in reference [63] shows that the cited critique of MCT is unjustified. The fitting of glycerol spectra by $\chi_{\text{int}}''(\omega)$ in reference [94] led to the conclusion that strong deviations from the MCT predictions have been found for this system. Depolarized light scattering spectra of glycerol have also been obtained by application of a tandem Fabry–Pérot spectrometer [74], and the window studied in this paper is two orders of magnitude larger than the one studied in reference [94]. In this work it is concluded that the data are consistent with MCT, but that the critical spectrum for those temperatures where a spectral minimum can be detected is masked by the transient spectrum. The conclusions of reference [94] have been invalidated and the interpretation of reference [74] was corroborated by showing that the solutions of a MCT model can describe the evolution of the structural relaxation of glycerol for frequencies between 0.4 GHz and 1 THz [95].

The third example of an empirical fit is obtained by considering stretched-relaxation spectra in a one-decade frequency window adjacent to the microscopic-excitation band, say the toluene results shown in figure 16 between 40 and 400 GHz. An interpolation of the results with a straight line is possible, i.e. the data can be fitted with a power law $\chi''(\omega) \propto \omega^{a(T)}$. The fit exponent $a(T)$ increases with decreasing temperature. Such a fit result must not be considered as an objection against the MCT prediction for a critical spectrum, specified by a temperature-independent exponent $a \leqslant a_{\max}$. On the contrary, even the leading-order asymptotic formula for the β-relaxation, whose application for a description of the data in figure 16 was demonstrated in reference [58], describes the experiments. The first scaling law implies that the coefficient $a(T)$, defined for a fixed frequency interval, increases with decreasing $T - T_c$. For positive $T - T_c$ one gets $a(T) < a$, for $T = T_c$ one finds $a(T_c) = a$, and for T falling below T_c the effective exponent increases towards unity. This holds, provided that there are no disturbances by the transient spectra. If these are present, as discussed in the preceding paragraph for glycerol, $a(T)$ may even rise above 1.

7.3. The $T < T_c$ problems

The most subtle results reviewed in this paper for conventional systems concern the evolution of the α-process within the GHz window and its interplay with the β-process as observed for $T > T_c$. The characteristic temperature T_c was obtained by scaling-law analysis of spectra measured for $T > T_c$ and in addition by detecting the Debye–Waller-factor anomaly for $T < T_c$. The solutions of schematic MCT models can also be used to describe the evolution of the depolarized light scattering spectra of CKN [96], Salol [96], and OTP [97]. These descriptions imply a complete fit of the α-peak, of the β-spectrum, and of parts of the microscopic-excitation band.

The status of the tests of spectra for $T < T_c$ is not clear at present mainly for two reasons. These spectra are modified seriously by activated transport processes which are ignored in the basic version of MCT; the activated processes are included approximately in the more complicated extended MCT only. The first problem is that a microscopical quantification of these activated processes and an evaluation of their effect on the solutions of the extended equations of motion is not available. The only result known so far is that for sufficiently small hopping effects equations (4) remain valid with the β-correlator generalized to a two-parameter scaling law. The activated processes enter as a single parameter δ which is called the hopping parameter. At present one can only try fits of data using δ as an adjustable number. The glassy dynamics has been analysed within the $\delta \neq 0$ β-relaxation theory for the depolarized light scattering spectra of CKN and Salol [68], PC [54], and OTP [63], as well as for Monte Carlo simulation results for a polymer model [35]. The position and the shape of the susceptibility minimum is influenced sensitively for $T < T_c$ by δ. Therefore a fit of δ should be made to this clearly distinguishable dynamical feature and a fit should be judged by the quality of such a study. This leads to the second problem: so far it has not been possible to measure the spectral minima for $T < T_c$. This renders the cited estimate of δ not compelling, as was emphasized in reference [68].

The absence of a reliable determination of δ has implications for a reliable description of other features of the $T < T_c$ spectra, for example the so-called susceptibility knee. This feature is present in the master spectrum $\hat{\chi}_+(\hat{\omega})$ of the β-process in the ideal MCT for the following reason. The correlator $g_+(\hat{t})$ in equation (5*b*) describes the crossover from critical decay for $\hat{t} \ll 1$ to arrest for $\hat{t} \gg 1$, as was discussed above for the hard-sphere-colloid results in connection with the lower panel of figure 5. This crossover leads to a corresponding one at some knee frequency $\omega_K \propto 1/t_\sigma$ for the spectrum from the regular variation for low

frequencies, $\hat{\chi}_+(\hat{\omega} \ll 1) \propto \hat{\omega}$, to the critical variation for high frequencies, $\hat{\chi}_+(\hat{\omega} \gg 1) \propto \hat{\omega}^a$. If δ is sufficiently small, the ideal spectrum will not be disturbed too much and the knee should be present. However, if δ is so large that the α-decay of the correlator starts for a time smaller than t_σ, the spectral knee will be absent. The depolarized light scattering spectra of Salol [47] and PC [54] did not exhibit a knee in the GHz window, and therefore the cited $\delta \neq 0$ fits had to use a sufficiently large hopping parameter. The OTP spectra, measured in a backward-scattering configuration [63], did not exhibit a knee either. But OTP spectra, measured in a 90°-scattering arrangement, did exhibit a knee-like structure and it was reported to be consistent with the MCT predictions [84]. However, for 90°-scattering experiments there appear transverse sound excitations in the spectral range of interest, and it is unclear how these modify the relaxation spectra to be analysed. The data for CKN were initially found to exhibit a knee [50]. But it was argued [98] that the depolarized light scattering spectra published so far, obtained by the tandem Fabry–Pérot spectrometer for the lowest frequencies and intensities, are invalidated by some parasitic white-noise-background spectrum. Therefore the spectra for $T \leqslant T_c$ have to be remeasured and reanalysed before a conclusion on the status of $\delta \neq 0$ fits can be drawn. For this reason, $T < T_c$ scaling-law fit results for scattering spectra have not been reviewed in section 4.

7.4. Associated and covalently bonded liquids

In a dense simple liquid a particle is located in a cage formed by its 11 to 13 nearest neighbours. MCT aims at a self-consistent treatment of the dynamics for the particle and its cage. Therefore one might hesitate to apply the theory in a discussion of network-forming liquids which have a much lower coordination number and where the significance of the cage effect is not so obvious. However, the general MCT results are universal and they reflect only a topologically stable singularity in the space of constants describing the coupling of density fluctuations. Therefore it is not impossible that the universal results are relevant also for the glassy dynamics of complex liquids, and it makes sense to examine whether or not the data for correlation functions and spectra show the typical MCT features. Indeed, as mentioned above, the simulation data for a simple point-charge model of water reproduce the open network structure of this liquid, and the data for the dynamics can be interpreted consistently within the MCT scenario; the critical temperature T_c can be identified reasonably well [41, 43–46]. A semi-schematic model for the description of molecular liquids has been introduced, which treats water as a simple liquid and accounts for the ignored rotational degrees of freedom by renormalizing the mode-coupling constants with a factor. The latter is fitted such that the critical temperature is reproduced. This model predicts the critical exponents correctly and describes the wave-vector dependence of the α-process for the centre-of-mass correlators reasonably well [99]. The simulation work as well as the analysis of Raman-scattering experiments [42] show that in the currently-accessible temperature range the critical decay law of water is masked by oscillation dynamics. Therefore a test of the first-scaling-law predictions is not yet possible. Also, for the other hydrogen-bonded liquid studied so far, glycerol, the low-frequency spectra due to oscillation dynamics interfere strongly with the relaxation spectra. But the light scattering spectra exhibit a critical decay law $\phi''(\omega) \propto 1/\omega^{1-a}$, $a \sim 0.3$, which for $T \sim 230$ K extends over the window between 1 and 100 GHz [74]. The neutron scattering work corroborates this finding [100]. A fit of the data with MCT results is possible, but did not lead to a compelling estimate of T_c [95].

The interactions in a multicomponent Zr-based metallic alloy, whose dynamics was studied by incoherent neutron spectroscopy, are partly of covalent nature. The correlators $\phi_q(t)$ have been studied for times between about 0.2 ps and 8 ps, and this for the wave-vectors 1.4, 1.6, 1.8, and 2.0 Å^{-1}. The data for temperatures between 1020 and 1200 K could be described with

high accuracy by the β-relaxation scaling law, equations (4*a*), (5*a*), yielding $\lambda = 0.77 \pm 0.04$ and $T_c = 875 \pm 6$ K [101]. Another system for which covalent bonding is important is $N_{0.5}Li_{0.5}PO_3$. The incoherent neutron scattering cross section obeyed the factorization property for the whole dynamical window studied [102]. It was shown that the spectra between 30 GHz and 1 THz and temperatures between 539 K and 773 K can be described well by the solutions of a schematic MCT model [103].

B_2O_3 is an extensively studied glass-forming system with a network structure due to covalent bonding. Density correlators $\phi_q(t)$ for a fixed wave-vector were measured by photon-correlation spectroscopy for temperatures between 506 and 543 K [104]. The data for a seven-decade dynamical window could be described by the MCT β-relaxation results. They describe the temperature-independent critical decay, which was detected over a two-decade window. Also the initial part of the α-process, which exhibits the von Schweidler law over a two-decade window, is evident in the data. These results indicate a critical temperature below 506 K, i.e. below $T_g \approx 523$ K. Unfortunately, it was not reported whether the scales for a β-relaxation scaling-law analysis follow the power-law predictions. Depolarized light scattering spectra have been analysed for B_2O_3 for frequencies above about 0.4 GHz. The band of microscopic excitations influences the spectra down to rather low frequencies. The susceptibility minimum was described by the interpolation formula $\chi''_{\rm int}(\omega)$ from section 7.2 [105]. The non-ergodicity parameters deduced from light scattering data [105] or from neutron scattering spectra [106] exhibit an anomaly which suggests a washed-out crossover at some critical temperature T_c between 700 K and 900 K. This value is not consistent with the cited photon-correlation data, and therefore it is unclear whether MCT can be applied to interpret the data for B_2O_3.

8. Concluding remarks

The anomalous dynamics of glass-forming liquids has been studied for more than a century for timescales larger than a nanosecond, i.e. for times exceeding the ones characteristic for conventional condensed-matter dynamics by at least a factor of 100. However, an understanding of glassy dynamics did not result from that work. Therefore it appears obvious to search for insight into the problem by analysing how the glassy dynamics evolves from the normal-state-liquid dynamics upon cooling or compressing the system. An additional motivation for such research was provided by the mode-coupling theory (MCT) for the evolution of structural relaxation in simple liquids. The specified studies by experiment and by molecular dynamics simulations require the determination of correlation functions or spectra within dynamical windows which extend those of conventional condensed-matter physics by several orders of magnitude, and this became feasible only during the past decade. Indeed, this modern work uncovered a whole series of previously unexpected features of glassy dynamics. This article reviews the parts of these new findings which were published during the past seven years and which were used by the authors for an assessment of the MCT. In the cited papers one can find more than 300 diagrams confronting data with some MCT prediction. From this stock of information 24 figures have been reproduced in order to illustrate various facets of the problem and to show representative examples for the many other comparisons between experimental results and simulation data with MCT mentioned in this review. This procedure should give a suitable impression of the present status of the discussion and stimulate the reader to study the original publications.

The work reviewed in the preceding sections has shown that the universal leading-order asymptotic MCT results provide a complete semi-quantitative description of the evolution of structural relaxation within the GHz band for some extensively studied typical glass-forming systems like the mixed salt CKN [1–3, 14, 16–18, 37, 50, 67–69, 93, 96] and the van der Waals

liquid OTP [4, 5, 15, 60–63, 73, 77, 84, 86, 97]. The structure relates to the distribution of the particles in space, and neutron scattering is the only technique which can measure this distribution for short and intermediate distances as well as its changes with increasing time. Therefore neutron scattering spectroscopy plays a distinguished role in the unfolding of the story of structural relaxation in the above-mentioned systems. But only the combination with the other experimental techniques mentioned in this article has been able to compensate for the shortcoming of neutron scattering spectroscopy, namely small dynamical windows. The crucial role of the crossover temperature T_c has been established for several systems, but further work is necessary to specify the limits of MCT as regards a description of the dynamics for temperatures below T_c. If it were to be possible to extend the accessible dynamical windows, one could also test MCT predictions which go beyond leading-order asymptotic results.

The microscopical understanding of normal-liquid dynamics owes much to the achievements of computer simulation studies, and this review makes it evident that this technique also provided essential information on the glassy dynamics. The α-process for temperatures above T_c has been analysed for several systems and many probing variables. The factorization property in the β-regime was demonstrated for several models and correlation functions. The cited comparisons of simulation results for a Lennard-Jones mixture with first-principles MCT calculation results provide strong support for the theory. Motivation for further studies of the range of validity of asymptotic MCT formulae and for extensions of the theory to systems of non-spherical molecules was provided by the discovery that the simulation results for water exhibit α-scale coupling for all correlations analysed, while the ones for the cited mixture and for a model of linear molecules do not. The analysis of simulation data and of experiments within the concepts provided by MCT identified a challenging problem for future simulation work: what models exhibit the critical decay as clearly as one knows it to be exhibited by several conventional systems? One might suspect that the crucial aspect of the problem is the interplay of the transient dynamics with structural relaxation, and more data on this phenomenon would guide MCT studies towards a solution.

The hard-sphere system has regularly been used as a paradigm for a simple liquid, and the experiments on hard-sphere colloids show that it can also serve as the simplest example of a system exhibiting glassy dynamics. For this system the ideal glass transition in the sense of MCT appears to be identical with the calorimetric glass transition, $\varphi_c = \varphi_g$. Hence the experimental and theoretical studies of the colloid are also relevant for establishing an understanding of the conventional glass transition. The cited work [10,27,32,33,72,76,81,82, 89] suggests that MCT explains the evolution of structural relaxation qualitatively correctly for packing fractions φ below and above the critical value φ_c, and that it provides a first-principles description of the data on a 15% accuracy level. There are some open questions whose answers would deepen our understanding of the glass transition problem and sharpen the assessment of MCT. First, it is unclear how hydrodynamic interactions, which enter the MCT results on structural relaxation via the timescale t_0 only, influence the crossover from the transient dynamics to the glassy dynamics. Molecular dynamics studies for the hard-sphere system without hydrodynamic interactions could be very informative in this context. Second, as a step towards a quantitative understanding of the influence of polydispersity on glassy dynamics, it would be helpful to analyse a binary mixture of spheres of different diameters. As a result, one could obtain data to use in testing how MCT can deal with those correlations which are different from the ones for the total-density fluctuations studied so far. The third problem is a special limiting case of the mixture problem. MCT predicts that the mean squared displacement dynamics of the hard-sphere system is different from the dynamics studied so far for other variables in the sense that leading-order β-relaxation results do not describe quantitatively the solutions of the full MCT equations in the parameter range of interest. Thus

a quantitative analysis of the mean squared displacement results would provide a new type of test of MCT.

MCT was constructed as a microscopical approach towards the dynamics of liquids. The cited comparisons of data for form factors and for exponent parameters with first-principles calculations done for the hard-sphere system and for the binary Lennard-Jones system show that this claim has some justification. There are a number of other systems for which detailed calculations and comparisons with data appear possible, for example charge-stabilized colloids. However, it is unclear whether first-principles calculations are feasible for the complicated conventional glass-forming liquids like CKN and OTP. Therefore it is of importance that MCT provides some general results for the evolution of glassy dynamics. These are based on leading-order asymptotic expansions near the glass transition singularity. They explain some general features shared e.g. by the molten salt CKN and a hard-sphere-colloidal suspension, and they justify the characterization of the anomalous dynamics studied by the same phrase 'structural relaxation'. But one faces a severe problem with the applicability of the above-mentioned general asymptotic results: there is no *a priori* quantitative specification of their range of validity. Within the ideal MCT the range of validity of the general formulae discussed on the preceding pages can be determined and the qualitative trends of the deviations from these leading-order results can be specified by calculating the leading corrections to the leading-order asymptotic results. This programme has been carried out recently for simple systems, and the results have been discussed in detail for the hard-sphere model [107, 108]. There are some general findings. The range of validity of the α-scaling law is bigger than that of the β-scaling law since corrections to the former are proportional to $\epsilon = (T - T_c)/T_c$ while those to the latter are proportional to $\sqrt{|\epsilon|}$. The dynamical window for the β-scaling law is larger in the $\log t$ than in the $\log \omega$ domain. There are relations between the corrections for small rescaled times $\hat{t} = t/t_\sigma$ and the ones for large $\hat{t}$, etc. Future work will show whether these findings are helpful for tests of MCT. The range of validity of some asymptotic law depends not only on the law considered but also on the variable A whose correlator or spectrum is studied. For example, for a wave-vector near the structure factor peak position, the range of validity of the t^{-a}-law for the decay towards the plateau is much smaller than that for a wave-vector near the first minimum of the structure factor. Von Schweidler's law describes a reasonable part of the α-process of the mean squared displacement, while the critical decay law is not detectable for this quantity within the range of parameters of interest in present simulation studies. The corrections to the asymptotic laws for the non-Gaussian parameter are so big that the two-step-relaxation scenario does not show up in the numerical solutions for reasonable values of $|\epsilon|$. To decide on the quantitative implications of the corrections, one has to evaluate a set of A-specific correction amplitudes in addition to two constants ξ and η. The latter are the analogues of λ and they fix the master functions determining the corrections to the leading-order results. But the evaluation of these constants and amplitudes requires the knowledge of the mode-coupling functional for the system under discussion, and such knowledge is not available for complicated systems. In addition to the above-described problems, there are the problems of the crossover from the transient to structural relaxation and the crossover from the cage-effect-dominated dynamics to activated transport. These crossovers imply deviations from the formulae discussed in this review, which are not sufficiently well understood. Because of the problems indicated, it would be premature to formulate a conclusion as to whether, e.g., the discrepancies between the values of T_c, reported by different authors for PC, or the deviations of the spectra in the β-relaxation window, found by dielectric-loss spectroscopy and light scattering, are due to failures of MCT or due to the corrections to leading-order results.

I hope that this review shows that the recent studies of an ancient problem of condensed-matter physics by experiment, simulation, and theory have been worthwhile, and that extensions

and improvements to these studies are rewarding.

Acknowledgments

I thank Herman Cummins very much for many discussions and suggestions. I thank him as well as M Fuchs, M Mayr, and J Wuttke for critical readings of the manuscript. I acknowledge gratefully the permission given by the authors of the papers quoted in the figure captions to reproduce their diagrams. The work was supported in part by Verbundprojekt BMBF 03-GO5TUM.

References

[1] Mezei F, Knaak W and Farago B 1987 *Phys. Scr.* T **19** 363
[2] Knaak W, Mezei F and Farago B 1988 *Europhys. Lett.* **7** 529
[3] Tao N J, Li G and Cummins H Z 1991 *Phys. Rev. Lett.* **66** 1334
[4] Bartsch E, Kiebel M, Fujara F, Sillescu H and Petry W 1989 *Dynamics of Disordered Materials* ed D Richter, A J Dianoux, W Petry and J Teixeira (Berlin: Springer) p 135
[5] Petry W, Bartsch E, Fujara F, Kiebel M, Sillescu H and Farago B 1991 *Z. Phys.* B **83** 175
[6] Roux J N, Barrat J-L and Hansen J-P 1989 *J. Phys.: Condens. Matter* **1** 7171
[7] Barrat J-L, Roux J N and Hansen J-P 1990 *Chem. Phys.* **149** 197
[8] Signorini G F, Barrat J-L and Klein M L 1990 *J. Chem. Phys.* **92** 1294
[9] Sjögren L 1991 *J. Phys.: Condens. Matter* **3** 5023
[10] van Megen W and Pusey P N 1991 *Phys. Rev.* A **43** 5429
[11] Götze W and Sjögren L 1992 *Rep. Prog. Phys.* **55** 241
[12] Götze W and Vujičić G M 1989 *Z. Phys.* B **76** 175
[13] Frick B, Farago B and Richter D 1990 *Phys. Rev. Lett.* **64** 2921
[14] Li G, Du W M, Hernandez J and Cummins H Z 1993 *Phys. Rev.* E **48** 1192
[15] Tölle A, Schober H, Wuttke J and Fujara F 1997 *Phys. Rev.* E **56** 809
[16] Yang Y and Nelson K A 1996 *J. Chem. Phys.* **104** 5429
[17] Kartini E, Collins M F, Collier B, Mezei F and Svensson E C 1996 *Phys. Rev.* B **54** 6292
[18] Pimenov A, Lunkenheimer P, Rall H, Kohlhaas R, Loidl A and Böhmer R 1996 *Phys. Rev.* E **54** 676
[19] Toulouse J, Coddens G and Pattnaik R 1993 *Physica* A **201** 305
[20] Yang Y and Nelson K A 1995 *Phys. Rev. Lett.* **74** 4883
[21] Yang Y, Muller L J and Nelson K A 1996 *Mater. Res. Soc. Symp. Proc.* **407** 145
[22] Börjesson L, Elmroth M and Torell L 1990 *Chem. Phys.* **149** 209
[23] Wahnström G 1991 *Phys. Rev.* A **44** 3752
[24] Lewis L J and Wahnström G 1993 *Solid State Commun.* **86** 295
[25] Lewis L J and Wahnström G 1994 *Phys. Rev.* E **50** 3865
[26] Pusey P N 1991 *Liquids, Freezing and Glass Transition (Les Houches)* ed J-P Hansen, D Levesque and J Zinn-Justin (Amsterdam: North-Holland) p 763
[27] van Megen W and Underwood S M 1993 *Phys. Rev. Lett.* **70** 2766
[28] Kob W and Andersen H C 1994 *Phys. Rev. Lett.* **73** 1376
[29] Kob W and Andersen H C 1995 *Phys. Rev.* E **51** 4626
[30] Kob W and Andersen H C 1995 *Phys. Rev.* E **52** 4134
[31] Nauroth M and Kob W 1997 *Phys. Rev.* E **55** 657
[32] van Megen W and Underwood S M 1993 *Phys. Rev.* E **47** 248
[33] van Megen W and Underwood S M 1994 *Phys. Rev.* E **49** 4206
[34] Baschnagel J 1994 *Phys. Rev.* B **49** 135
[35] Baschnagel J and Fuchs M 1995 *J. Phys.: Condens. Matter* **7** 6761
[36] Gleim T, Kob W and Binder K 1998 *Phys. Rev. Lett.* **81** 4404
[37] Lunkenheimer P, Pimenov A and Loidl A 1997 *Phys. Rev. Lett.* **78** 2995
[38] Kämmerer S, Kob W and Schilling R 1997 *Phys. Rev.* E **56** 5450
[39] Kämmerer S, Kob W and Schilling R 1998 *Phys. Rev.* E **58** 2131
[40] Kämmerer S, Kob W and Schilling R 1998 *Phys. Rev.* E **58** 2141
[41] Sciortino F, Fabbian L and Tartaglia P 1998 *Nuovo Cimento* D **20**
[42] Sokolov A P, Hurst J and Quitmann D 1995 *Phys. Rev.* B **51** 12 865

[43] Gallo P, Sciortino F, Tartaglia P and Chen S-H 1996 *Phys. Rev. Lett.* **76** 2730
[44] Sciortino F, Gallo P, Tartaglia P and Chen S-H 1996 *Phys. Rev.* E **54** 6331
[45] Sciortino F, Fabbian L, Chen S-H and Tartaglia P 1997 *Phys. Rev.* E **56** 5397
[46] Fabbian L, Sciortino F and Tartaglia P 1998 *J. Non-Cryst. Solids* **235–237** 325
[47] Li G, Du W M, Sakai A and Cummins H Z 1992 *Phys. Rev.* A **46** 3343
[48] Torre R, Bartolini P and Pick R M 1998 *Phys. Rev.* E **57** 1912
[49] Halalay I C and Nelson K A 1992 *Phys. Rev. Lett.* **69** 636
[50] Li G, Du W M, Chen X K, Cummins H Z and Tao N J 1992 *Phys. Rev.* A **45** 3867
[51] Bartsch E, Antonietti M, Schupp W and Sillescu H 1992 *J. Chem. Phys.* **97** 3950
[52] Toulouse J, Pick R and Dreyfus C 1996 *Mater. Res. Soc. Symp. Proc.* **407** 161
[53] Lunkenheimer P, Pimenov A, Dressel M, Gorshunov B, Schneider U, Schiener B, Böhmer R and Loidl A 1997 *Mater. Res. Soc. Symp. Proc.* **455** 47
[54] Du W M, Li G, Cummins H Z, Fuchs M, Toulouse J and Knauss L A 1994 *Phys. Rev.* E **49** 2192
[55] Lunkenheimer P, Pimenov A, Dressel M, Schiener B, Schneider U and Loidl A 1997 *Prog. Theor. Phys. Suppl.* **126** 123
[56] Ma J, Bout D V and Berg M 1996 *Phys. Rev.* E **54** 2786
[57] Rössler E, Sokolov A P, Eiermann P and Warschewske U 1993 *Physica* A **201** 237
[58] Wuttke J, Seidl M, Hinze G, Tölle A, Petry W and Coddens G 1998 *Eur. Phys. J.* B **1** 169
[59] Li G, King H E Jr, Oliver W F, Herbst C A and Cummins H Z 1995 *Phys. Rev. Lett.* **74** 2280
[60] Wuttke J, Kiebel M, Bartsch E, Fujara F, Petry W and Sillescu H 1993 *Z. Phys.* B **91** 357
[61] Bartsch E 1995 *J. Non-Cryst. Solids* **192–193** 384
[62] Tölle A, Schober H, Wuttke J, Randl O G and Fujara F 1998 *Phys. Rev. Lett.* **80** 2374
[63] Cummins H Z, Li G, Du W, Hwang Y H and Shen G Q 1997 *Prog. Theor. Phys. Suppl.* **126** 21
[64] Wahnström G and Lewis L J 1997 *Prog. Theor. Phys. Suppl* **126** 261
[65] Bartsch E 1995 *Transport Theory Stat. Phys.* **24** 1125
[66] Bartsch E, Frenz V, Baschnagel J, Schärtl W and Sillescu H 1997 *J. Chem. Phys.* **106** 3743
[67] Mezei F 1991 *Ber. Bunsenges. Phys. Chem.* **95** 1118
[68] Cummins H Z, Du W M, Fuchs M, Götze W, Hildebrand S, Latz A, Li G and Tao N J 1993 *Phys. Rev.* E **47** 4223
[69] Fuchs M, Cummins H Z, Du W M, Götze W, Latz A, Li G and Tao N J 1995 *Phil. Mag.* B **71** 771
[70] Mezei F 1992 *Slow Dynamics in Condensed Matter (AIP Conf. Proc. 256)* (New York: American Institute of Physics) p 53
[71] Fuchs M 1994 *J. Non-Cryst. Solids* **172–174** 241
[72] van Megen W 1995 *Transport Theory Stat. Phys.* **24** 1017
[73] Tölle A, Wuttke J, Schober H, Randl O G and Fujara F 1998 *Eur. Phys. J.* B **5** 231
[74] Wuttke J, Hernandez J, Li G, Coddens G, Cummins H Z, Fujara F, Petry W and Sillescu H 1994 *Phys. Rev. Lett.* **72** 3052
[75] Lunkenheimer P, Pimenov A, Dressel M, Yu Goncharov G, Böhmer R and Loidl A 1996 *Phys. Rev. Lett.* **77** 318
[76] van Megen W, Mortensen T C, Müller J and Williams S R 1998 *Phys. Rev.* E **58** 6073
[77] Lohfink M and Sillescu H 1992 *Slow Dynamics in Condensed Matter (AIP Conf. Proc. 256)* (New York: American Institute of Physics) p 30
[78] Fujara F, Geil B, Sillescu H and Fleischer G 1992 *Z. Phys.* B **88** 195
[79] Chang I and Sillescu H 1997 *J. Phys. Chem.* B **101** 8794
[80] Segrè P N, Meeker S P, Pusey P N and Poon W C K 1995 *Phys. Rev. Lett.* **75** 958
[81] van Megen W and Underwood S 1994 *Phys. Rev. Lett.* **72** 1773
[82] Mason T G and Weitz D A 1995 *Phys. Rev. Lett.* **75** 2770
[83] Sölken St, Bartsch E, Sillescu H and Lindner P 1995 *Prog. Colloid Polym. Sci.* **98** 155
[84] Steffen W, Patkowski A, Gläser H, Meier G and Fischer E W 1994 *Phys. Rev.* E **49** 2992
[85] Patkowski A, Steffen W, Meier G and Fischer E W 1994 *J. Non-Cryst. Solids* **172–174** 52
[86] Cummins H Z, Hwang Y H, Li G, Du W M, Losert W and Shen G Q 1998 *J. Non-Cryst. Solids* **235–237** 254
[87] Bartsch E, Bertagnolli H, Chieux P, David A and Sillescu H 1993 *Chem. Phys.* **169** 373
[88] Kartini E, Collins M F, Collier B, Mezei F and Svensson E C 1995 *Can. J. Phys.* **73** 748
[89] Henderson S I and van Megen W 1998 *Phys. Rev. Lett.* **80** 877
[90] Bernu B, Hansen J-P, Hiwatari Y and Pastore G 1987 *Phys. Rev.* A **36** 4891
[91] Löwen H, Hansen J-P and Roux J N 1991 *Phys. Rev.* A **44** 1169
[92] Fuchs M, Götze W, Hildebrand S and Latz A 1992 *Z. Phys.* B **87** 43
[93] Cummins H Z, Li G, Du W M, Hernandez J and Tao N J 1995 *Transport Theory Stat. Phys.* **24** 981

[94] Sokolov A P, Steffen W and Rössler E 1995 *Phys. Rev.* E **52** 5105
[95] Franosch T, Götze W, Mayr M R and Singh A P 1997 *Phys. Rev.* E **55** 3183
[96] Krakoviack V, Alba-Simionesco C and Krauzmann M 1997 *J. Chem. Phys.* **107** 3417
[97] Singh A P, Li G, Götze W, Fuchs M, Franosch T and Cummins H Z 1998 *J. Non-Cryst. Solids* **235–237** 66
[98] Surovtsev N V, Wiedersich J A H, Novikov N V, Rössler E and Sokolov A P 1998 *Phys. Rev.* B **58** 14 888
[99] Fabbian L, Sciortino F, Thiery F and Tartaglia P 1998 *Phys. Rev.* E **57** 1485
[100] Wuttke J, Petry W, Coddens G and Fujara F 1995 *Phys. Rev.* E **52** 4026
[101] Meyer A, Wuttke J, Petry W, Randl O G and Schober H 1998 *Phys. Rev. Lett.* **80** 4454
[102] Rufflé B, Etrillard J, Toudic B, Ecolivet C, Coddens G, Ambroise J P, Gueguen E and Marchand R 1997 *Phys. Rev.* B **56** 11 546
[103] Rufflé B, Beaufils S, Toudic B, Ecolivet C, Le Sauce A and Marchand R 1998 *J. Non-Cryst. Solids* **235–237** 244
[104] Sidebottom D, Bergman R, Börjesson L and Torell L M 1993 *Phys. Rev. Lett.* **71** 2260
[105] Brodin A, Börjesson L, Engberg D, Torell L M and Sokolov A P 1996 *Phys. Rev.* B **53** 11 511
[106] Engberg D, Wischnewski A, Buchenau U, Börjesson L, Dianoux A J, Sokolov A P and Torell L M 1998 *Phys. Rev.* B **58** 9087
[107] Franosch T, Fuchs M, Götze W, Mayr M R and Singh A P 1997 *Phys. Rev.* E **55** 7153
[108] Fuchs M, Götze W and Mayr M R 1998 *Phys. Rev.* E **58** 3384